Seismic Tests of Beam-to-Column Connections in a Precast Concrete Frame

Sergio M. Alcocer, Ph.D.
Professor
Institute of Engineering
University of Mexico (UNAM)
and Director of Research
National Center for Disaster Prevention
(CENAPRED)
Mexico City, Mexico

Rene Carranza, S.E.
Director General
Servicios y Elementos Presforzados,
S.A. de C.V. (SEPSA)
Mexico City, Mexico

David Perez-Navarrete, M.Sc.
Former Graduate Student
School of Engineering
University of Mexico (UNAM)
Mexico City, Mexico

Raul Martinez, S.E.
Project Manager
Servicios y Elementos Presforzados,
S.A. de C.V. (SEPSA)
Mexico City, Mexico

Two full-scale beam-to-column connections in a precast concrete frame were tested under uni-directional and bi-directional cyclic loading that simulated earthquake-type motions. Variables included the detailing used at the joint to achieve structural continuity of the beam reinforcement, and the type of framing (whether two-dimensional or three-dimensional). The most relevant feature of the connection is that conventional mild steel reinforcing bars or prestressing strands, rather than welding or special bolts, were used to achieve beam continuity. Specimen design followed the strong-column–weak-beam concept. Beam reinforcement was purposely designed and detailed to develop hinges at the joint faces and to impose large inelastic shear force demands into the joint. During specimen fabrication, the joint details enabled ease and speed of construction. As expected, the joint controlled the specimen failure. In general, the performance of both beam-to-column connections was satisfactory. Joint strength was 80 percent of that expected for monolithic reinforced concrete construction. Specimen behavior was ductile due to hoop yielding and bar pullout, while strength was nearly constant up to drifts of 3.5 percent.

Precast concrete has been widely accepted as a viable means of constructing safe, durable, reliable, high-quality, and cost-effective structural systems. Its full implementation in high seismic areas, however, has been somewhat limited, mainly due to scarce design guidelines as compared to those available for cast-in-place concrete structures. In particular, the lack of design provisions for

seismic-resistant beam-to-column connections appropriate for precast concrete frame construction is still apparent in North America (Mexico, United States, and Canada).[1]

Another obstacle to the use of precast concrete construction in seismic areas has been the imposition of prescriptive provisions developed to promote ductility in cast-in-place concrete construction.[2] This set of design and detailing requirements makes a standard methodology for establishing equivalence of energy dissipation and ductility between precast concrete and cast-in-place systems desirable. In 1999, such a standard methodology was developed by an Innovation Task Group (ITG) of the American Concrete Institute, which was published.[3]

Two design approaches are available for the design of precast concrete lateral force-resisting systems.[4] Emulation of monolithic reinforced concrete construction is the approach most commonly adopted in codes.[5-7] The alternative approach is the use of the unique properties of the precast concrete elements interconnected by either dry or wet connections.[8]

In the past, some precast concrete framed structures have performed poorly in earthquakes because of inadequate connection details.[5] To gain confidence in the use of precast concrete in moment-resisting frames, satisfactory methods for connecting the precast elements together were required. Therefore, recommendations developed for the seismic design of cast-in-place systems were straightforwardly adapted – that is, the objective of the design method was to emulate monolithic construction.

The Mexico City Building Code (MCBC)[6] permits the use of precast concrete structural systems based on emulation of the behavior of monolithic cast-in-place concrete systems. Specific requirements on material properties, construction details, and design are given in the code.

The MCBC requires that the design compressive strength of the concrete used in the connection be equal to or greater than that of the adjoining elements. Steel reinforcement in the connection, either longitudinal or transverse, must have a nominal yield strength limited to 414 MPa (60 ksi). Typical Mexican reinforcing steel follows standards similar to ASTM A 615.

Fig. 1. Type of precast concrete frame construction studied.

Connections have to be designed and detailed to resist 1.3 times the forces and moments obtained from analysis that act at their boundaries. The 1.3 factor is in addition to the usual load factors. Finally, all surfaces of precast concrete elements in contact with the connections must be free of laitance, intentionally roughened to a full amplitude of 5 mm (0.2 in.), and saturated with water 24 hours prior to casting the concrete in the connection.

As is commonly done in other countries, the seismic-induced design forces recommended in the MCBC are significantly less than the inertia forces induced if the structure were to respond in the elastic range to a major earthquake. The design seismic-induced force is related to the achievable structural ductility through seismic response modification factors Q, which are equivalent to the force-reduction factors R in the Uniform Building Code.[7] Therefore, the MCBC

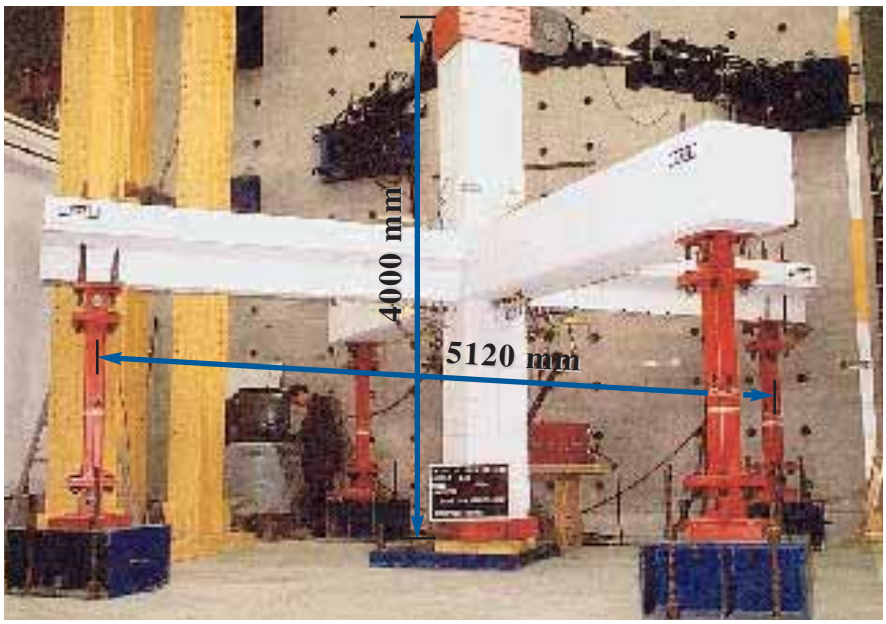

Fig. 2. Specimen geometry and testing rig.

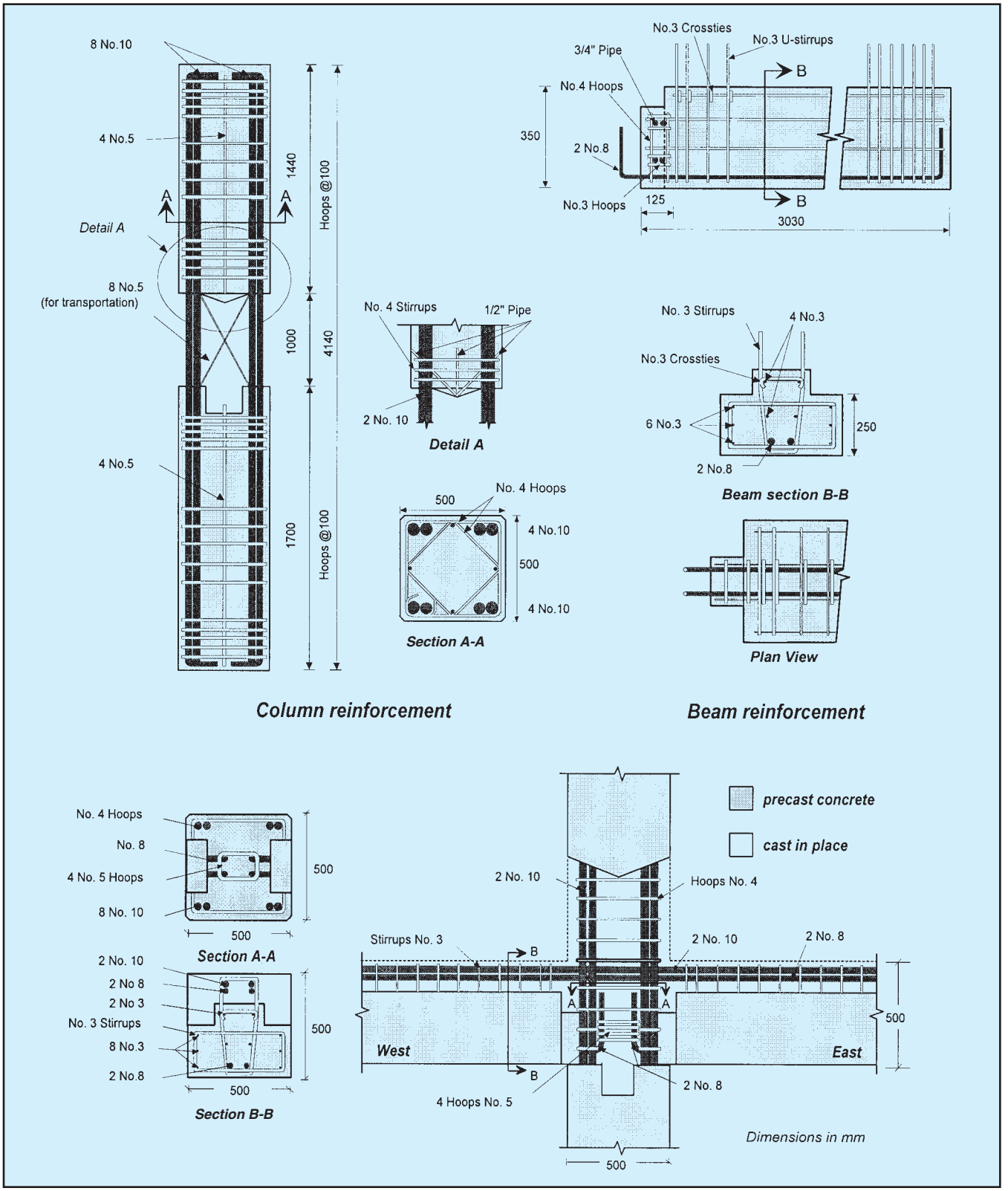

Fig. 3. Dimensions and detailing of Specimen J1.

design criterion is force-based.

For ductile moment-resisting cast-in-place frames, a Q value of 3 or 4 is used to determine the appropriate design load from elastic design spectra. However, for both values of the seismic response modification factors, the same detailing requirements apply. The choice of using a Q of 3 or 4 is left to the designer. The ultimate design horizontal seismic forces typically vary between 0.04g and 0.2g, depending on the seismic zone, the soil category, the importance of the structure, and the fundamental period of vibration of the structure. For precast concrete frames, a Q of 2 or 3 is used and the ultimate design horizontal

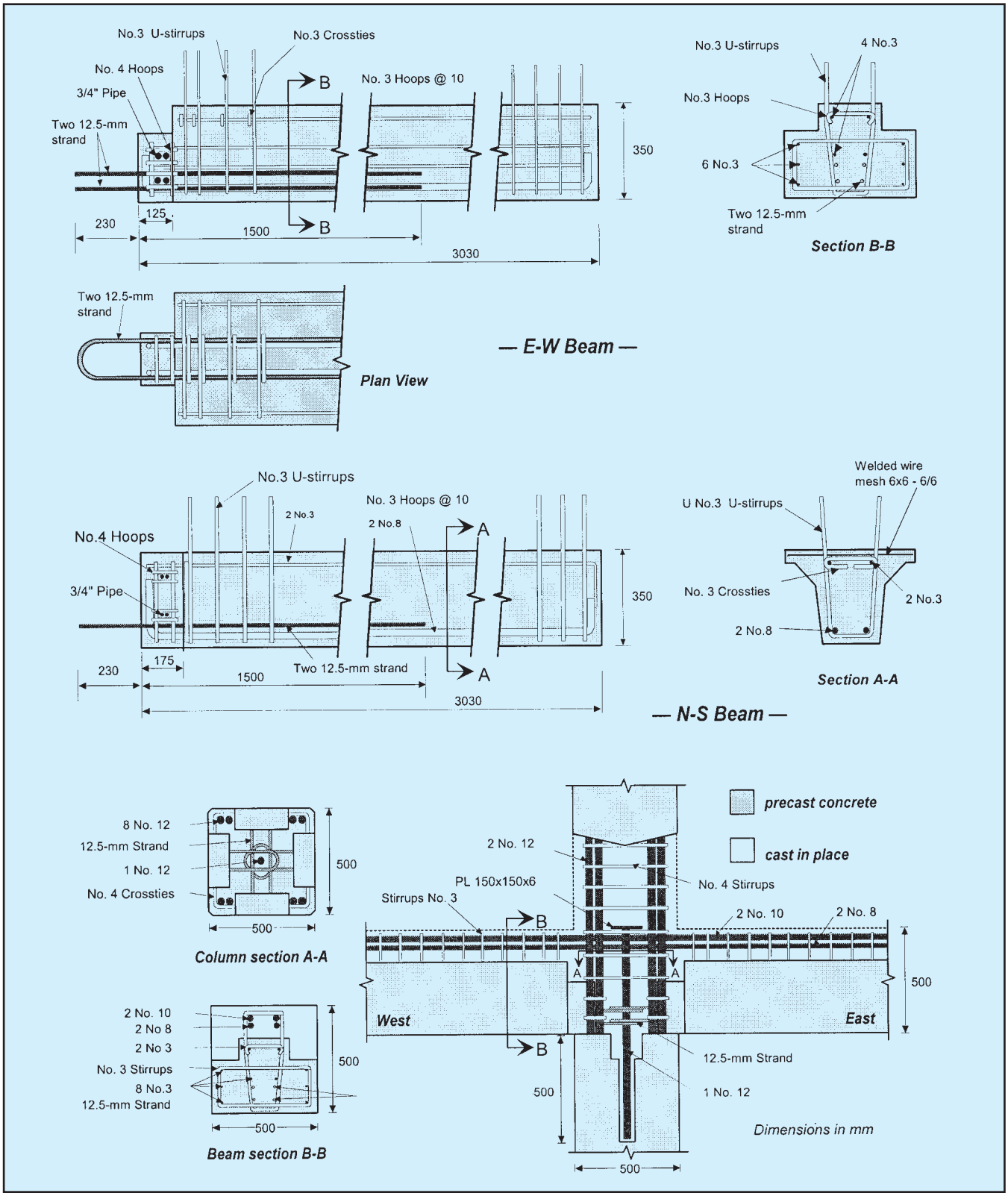

Fig. 4. Dimensions and detailing of Specimen J2.

seismic-induced forces vary between 0.04*g* and 0.3*g*.

As has been recognized,[5] the challenge in precast frame construction lies in finding economical and practical methods of connecting the precast concrete elements together to ensure adequate stiffness, strength, ductility and stability. A number of experimental research programs conducted in recent years have significantly improved our understanding of the behavior of connections between precast concrete elements.[9-18] For example, internal resisting mechanisms have been identified and understood,[10,14-16,18] and design and detailing requirements have been developed.[12,14,17,18]

Table 1. Material properties.

Element	Specimen J1	Specimen J2
Concrete, f'_c:		
Precast columns and beams	32 MPa (4650 psi)	42 MPa (6040 psi)
Cast-in-place joint	44 MPa (6370 psi)	40 MPa (5840 psi)
Prestressing steel, nominal, f_y:		
12.7 mm (0.5 in.) strand	N/A	1872 MPa (271,520 psi)
Reinforcing steel in precast elements:		
No. 3 (9.53 mm)		
f_y	411 MPa (59,660 psi)	456 MPa (66,140 psi)
f_u	716 MPa (103,830 psi)	713 MPa (103,400 psi)
Elongation at fracture	10.3 percent	8.0 percent
No. 4 (12.7 mm)		
f_y	437 MPa (63,440 psi)	424 MPa (61,510 psi)
f_u	700 MPa (101,550 psi)	684 MPa (99,130 psi)
Elongation at fracture	9.6 percent	9.2 percent
No. 5 (15.88 mm)		
f_y	434 MPa (63,010 psi)	413 MPa (59,880 psi)
f_u	691 MPa (100,270 psi)	678 MPa (98,280 psi)
Elongation at fracture	11.6 percent	10.4 percent
No. 8 (25.4 mm)		
f_y	455 MPa (65,990 psi)	454 MPa (65,850 psi)
f_u	719 MPa (104,250 psi)	698 MPa (101,270 psi)
Elongation at fracture	13.7 percent	12.3 percent
No. 10 (31.75 mm)		
f_y	441 MPa (64,000 psi)	N/A
f_u	726 MPa (105,250 psi)	N/A
Elongation at fracture	15.5 percent	N/A
No. 12 (38.1 mm)		
f_y	N/A	431 MPa (62,440 psi)
f_u	N/A	700 MPa (101,550 psi)
Elongation at fracture	N/A	18.3 percent
Reinforcing steel in cast-in-place concrete:		
No. 4 (12.7 mm)		
f_y	437 MPa (63,430 psi)	424 MPa (61,510 psi)
f_u	700 MPa (101,550 psi)	684 MPa (99,130 psi)
Elongation at fracture	9.6 percent	9.2 percent
No. 5 (15.88 mm)		
f_y	434 MPa (63,010 psi)	N/A
f_u	691 MPa (100,270 psi)	N/A
Elongation at fracture	11.6 percent	N/A
No. 6 (19.1 mm)		
f_y	N/A	420 MPa (60,870 psi)
f_u	N/A	668 MPa (96,860 psi)
Elongation at fracture	N/A	12.8 percent
No. 8 (25.4 mm)		
f_y	460 MPa (66,700 psi)	458 MPa (66,420 psi)
f_u	729 MPa (105,680 psi)	698 MPa (101,270 psi)
Elongation at fracture	13.0 percent	13.9 percent
No. 10 (31.75 mm)		
f_y	448 MPa (65,000 psi)	476 MPa (68,980 psi)
f_u	731 MPa (105,960 psi)	721 MPa (104,540 psi)
Elongation at fracture	12.7 percent	12.8 percent

Note: 1 in. = 25.4 mm; 1 psi = 0.006895 MPa.

In some research programs, precast elements have been connected at the beam-to-column joint region;[9-16,18] in others, elements have been connected at midspan (in the case of beams) and at midheight (in the case of columns).[15,16] Since one advantage of using one-way perimeter frames is the reduced complexity of the design and construction of the beam-to-column joints, many studies have focused on the performance of perimeter precast concrete frame joints.[9-17]

In emulation systems, precast beam longitudinal reinforcement that is connected at the beam-to-column joint is commonly spliced. Splicing can be achieved through proprietary steel sleeves[11,15,16] or by lap splicing bars, which may be bent to form 90-degree standard hooks.[16,17] In other cases, continuity at the joint has been achieved by means of bonded post-tensioning,[9] ungrouted post-tensioning,[10,14] or mild reinforcing steel bars grouted inside the joint but with an unbonded length adjacent to the column face.[13]

This paper reports on the behavior of concrete frames under cyclic loading of a precast concrete beam-to-column connection developed and used in Mexico. In the frame under consideration, design and detailing were aimed at emulating monolithic construction, as is required in the MCBC.[6] This investigation was conducted to assess the joint behavior and its stiffness, deformation, and strength characteristics when subjected to large shear and bond force demands. It was considered that such information would be useful in assessing the validity of the emulation hypothesis.

The beam-to-column connection discussed herein has already been used in Mexico for low-rise commercial buildings up to 25 m (82 ft) in height. The system consists of multistory precast concrete columns that have open gaps at each floor level (see Fig. 1). Typically, columns are fabricated in one piece and extend over a number of stories.

To form the gaps, concrete placement is interrupted at each floor level. These gaps allow placement of the precast beams during erection. To improve horizontal shear transfer at the joint, a 150 mm (5.9 in.) deep square hole is left in the concrete in the column below the joint. During placement of the joint concrete, concrete fills the hole so that it works as a shear key. Because the shear key is left unreinforced, its strength is limited to the shear strength of the concrete.

To promote the escape of the entrapped air in the joint concrete during casting and compacting, an inverted pyramid shape is formed in the precast column above the joint. In addition, a 12.7 mm (0.5 in.) diameter pipe that runs from the pyramid vertex up to one side of the precast column is left embedded.

Column longitudinal bars are made continuous through the gaps and are placed near the corners to leave ample free space for beam erection and placement. The column height is limited by the hauling truck's load capac-

ity and dimensions, as well as by highway and urban traffic regulations. If needed, the precast column units can be spliced at a floor midheight.

Single-bay precast beams, either prestressed or conventionally reinforced, are T- and inverted-T-beams. Beams are placed between columns and seated on the cover concrete and part of the core of the lower part of the precast concrete column. The bottom steel reinforcement protrudes from the beam ends and extends into the joint. This reinforcement may be bent to form either standard 90-degree hooks or closed loops.

A precast concrete hollow-core one-way floor system is placed on top of the inverted-T precast beam elements and spans between them, parallel to the T-beams. The reinforcement is then placed on top of the beam, in the topping slab over the floor system, and in the beam-to-column joint core. Finally, the concrete for the joint region and the topping slab is placed.

TEST PROGRAM

Two full-scale beam-to-column connections made with precast beams and columns were fabricated and tested. The specimens represented an interior joint of a lower story of a multistory building. The test units modeled the region from mid-column height below the joint to mid-column height above the joint and from midspan to midspan of beam on either side of the joint.

Specimen geometries are shown in Fig. 2; dimensions correspond to the distance between hinged supports. Dimensions and details of the test units are presented in Figs. 3 and 4. Test units consisted of beams 5.56 m (18.2 ft) long framing into a column 4.00 m (13.1 ft) high at midheight.

Experimental variables studied were the type of framing (two- and three-dimensional) and the joint detailing for continuity of beam reinforcement.[19,20] The intent of connecting the bottom bars was to transmit tensile forces to the far side of the joint so that a diagonal compression strut could form along the diagonal of the joint panel zone. Design concrete cover for all elements was 25 mm (1 in.) for both specimens.

Table 2. Member forces and strengths.

	Specimen J1	Specimen J2
Beam flexure		
Beam flexural strength M_p^+	281 kN-m (2480 kip-in.)	276 kN m (2440 kip-in.)
Beam flexural strength M_p^-	540 kN-m (4780 kip-in.)	579 kN m (5120 kip-in.)
Beam shear		
Shear corresponding to M_p	211 kN (47 kips)	226 kN (51 kips)
V_n (MCBC, beam)	431 kN (97 kips)	484 kN (109 kips)
Column flexure		
Axial force P	0	0
Moment corresponding to M_p	411 kN-m (3640 kip-in.)	428 kN-m (3780 kip-in.)
M_n (moment-curvature analysis)	579 kN-m (5120 kip-in.)	785 kN-m (6940 kip-in.)
Column shear		
Shear corresponding to M_p	235 kN (53 kips)	244 kN (55 kips)
V_n (MCBC, column)	633 kN (142 kips)	636 kN (143 kips)
Joint shear		
Horizontal shear force	1636 kN (368 kips)	1777 kN (399 kips)
Shear stress	6.5 MPa (949 psi)	7.1 MPa (1031 psi)
Shear strength $V_{n,j}$, γ=15 (ACI-ASCE Committee 352)	2530 kN (569 kips)	2442 kN (549 kips)
Shear strength $V_{n,j}$, γ=12 (ACI-ASCE Committee 352)	2070 kN (465 kips)	1998 kN (449 kips)
Maximum interstory drift applied, percent	3.5 percent	3.5 percent

Note: 1 psi = 0.006895 MPa; 1 kip = 4.448 kN; 1 kip-in. = 0.113 kN-m.

Specimen J1 consisted of two beams framing into the joint on opposite sides (2D construction); the bottom longitudinal steel reinforcement of the beams was terminated with 90-degree hooks at the joint. Continuity of this reinforcement through the joint was achieved with hoops placed around the extensions of the 90-degree hooks that protruded from the beam ends. Hoops had a 90-degree bend with an extension of six bar diameters.

The column of Specimen J1 was square with 500 mm (19.7 in.) sides and was reinforced with eight No. 10 (31.75 mm diameter) Grade 60 (f_y = 414 MPa or 60 ksi) continuous longitudinal bars and No. 4 (12.7 mm diameter) hoops at 100 mm (3.9 in.) spacing. The height of the gap in the column for beam placement and casting of the joint was 1000 mm (39.4 in.).

Specimen J1 had beams with a final 500 mm (19.7 in.) square section. The partially precast beams had an inverted-T shape and were reinforced with two No. 8 (25.4 mm diameter) bottom longitudinal bars and No. 3 (9.53 mm diameter) stirrups spaced at 100 mm (3.9 in.) on center. Bottom bars protruded from the beam ends into the joint with 90-degree hooks.

Additional No. 4 and No. 3 Grade 60 longitudinal bars were placed in the columns and beams to ease the fabrication of the cages. Since the beam width in the east-west direction was the same as the column width, a 250 mm (9.8 in.) reduction was made at the joint in order to fit the beam between the column longitudinal bundled bars (see Fig. 3).

Once the column and the beams were mounted on the test rig (see Fig. 2), the continuity reinforcement of the beam bottom longitudinal bars was placed. For Specimen J1, this reinforcement consisted of four No. 5 (15.88 mm diameter) Grade 60 hoops placed around the extensions of the 90-degree hooks.

Hoops were proportioned so that they would remain elastic while transferring the tensile axial force developed along the beam bottom reinforcement at ultimate bending moment. Since the nominal yield strengths of the hoop and longitudinal bars were the same, the total area of hoop legs in the direction of loading was 1.5 times the total area of beam bottom longitudinal bars.

To improve the confinement, strength, and deformability of the joint concrete, No. 4 cross-ties were placed around the joint through holes left across the beam width during precast fabrication. Several horizontal steel pipes were left embedded in the beams, at the design joint hoop spacing, to allow placement of joint hoops or cross-ties. Hoops were anchored

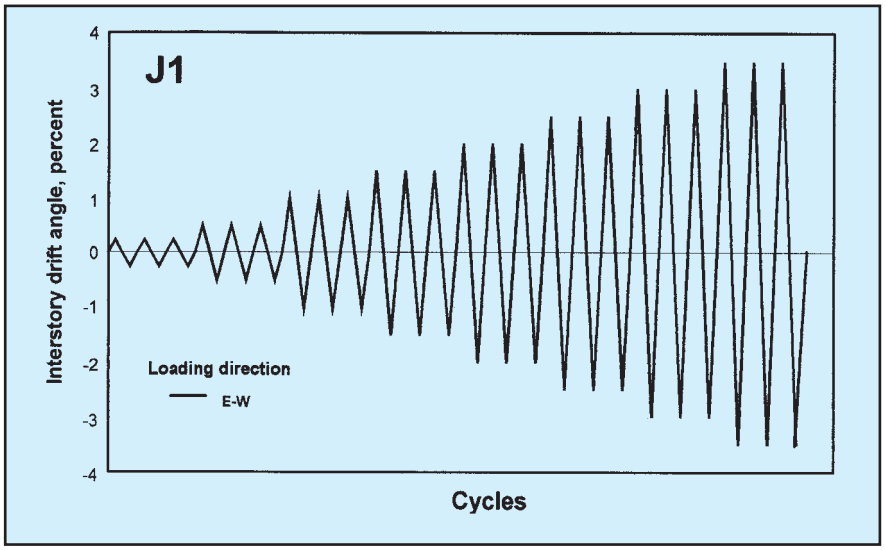

Fig. 5a. Displacement-controlled test sequence for Specimen J1.

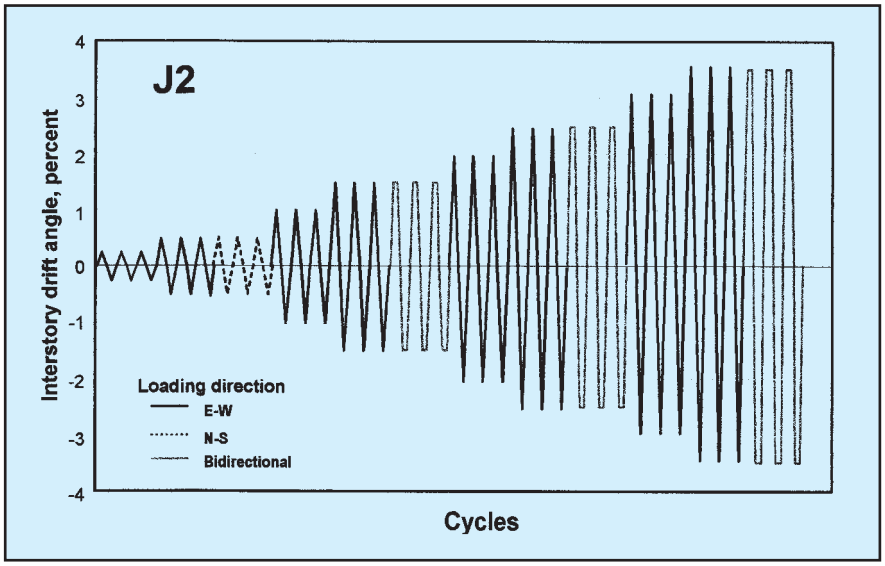

Fig. 5b. Displacement-controlled test sequence for Specimen J2.

around column longitudinal bars with alternating 90-degree and 135-degree hooks.

Afterwards, continuous beam top reinforcement was placed through the joint and the U-shaped beam stirrups, left anchored during precasting, were bent around. Beam top reinforcement consisted of two No. 8 and two No. 10 continuous bars (see Fig. 3). Finally, 40 MPa (5800 psi) ready-mixed concrete was placed in the joint and on top of the precast beams.

In Mexico, all frames of a building are typically designed to resist the seismic-induced forces. Therefore, frames are commonly designed and detailed as special moment-resisting frames (SMRFs). To examine the behavior of an interior joint of such a structural system layout, Specimen J2 was tested.

In Specimen J2, the bottom longitudinal reinforcement of the beam was interrupted at the joint face and lap-spliced with a U-shaped prestressing strand that extended from the beam into the joint. Continuity was achieved with a steel bolt inserted through the overlapping U-shaped prestressing strands at the joint mid-depth (see Fig. 4).

The Specimen J2 column had the same dimensions and transverse reinforcement as Specimen J1; however, continuous longitudinal reinforcement was made of eight No. 12 (38.1 mm diameter) Grade 60 bars. This bar size is readily available in Mexico.

In the east-west direction, beams were similar to those of Specimen J1. In the north-south direction, T-beams with a 200 x 500 mm (7.9 x 19.7 in.) cross section were used. These beams were reinforced similarly to east-west beams. In both the east-west and north-south beams, bottom longitudinal bars were interrupted at the joint (see Fig. 4).

To provide continuity to the beam bottom reinforcement, looped (U-shaped) prestressing strands were lap spliced 125 mm (4.9 in.) with the deformed longitudinal bars. A No. 12 Grade 60 bar was inserted vertically through the intersection of the looped (U-shaped) low-relaxation Grade 270 (f_y = 1860 MPa) prestressing strands that protruded from the beams; the bar was anchored inside the square column hole in the precast column below the joint.

To improve bar anchorage inside the joint, a square steel plate was butt-welded in the upper part; further analysis of strain gauge data indicated that the plate was not necessary.[20] Prestressing strands were designed to yield when conventional beam bottom bars yielded, i.e., when beam plastic hinges formed. The vertical steel bar was designed to remain elastic under yield demands from the strands at ultimate.

Similarly to Specimen J1, transverse reinforcement was provided to confine the joint concrete. No. 4 cross-ties were anchored around column longitudinal bars with 90-degree and 135-degree hooks, alternated over the joint height (see Fig. 4).

The beam top reinforcement in the east-west direction of Specimen J2 was the same as in Specimen J1. In the north-south direction of Specimen J2, two No. 8 and two No. 6 (19.1 mm diameter) bars were used.

To induce forces in the joint at levels near the shear strength, large beam moments had to be developed. For this to happen, it was necessary to use a large amount of beam steel area through the joint region. Because of space limitations, it was decided to use larger but fewer bars (two No. 8 and

two No. 10 bars), being cognizant that, especially for No. 10 bars, slippage and bond failure was more likely to occur. Moreover, the No. 10 bars did not comply with the minimum ratio of column depth to beam bar diameter. Analysis of strain gauge data indicated that bar slippage did not occur in either specimen.[19,20]

Specimens were built without the topped hollow-core slabs generally used in the system. It was assumed that since the hollow-core slab acted as a one-way floor system in the north-south direction of the specimens, its contribution to joint capacity was not significant.

Table 1 lists the unconfined compressive strength of the concrete found from cylinder tests at the time of testing the beam-to-column joint units, the yield and ultimate tensile strength, and elongation at fracture of various reinforcement sizes used. Concrete cylinders were cured in the same environment as specimens. Calculated member capacities are provided in Table 2, based on the measured material strengths listed in Table 1 and on measured bar locations. The member strengths do not include strength reduction factors.

The flexural strength M_p of the beam plastic hinges was based on the assumption that concrete would follow Hognestad's model. Column flexural strength, based on a moment-curvature analysis considering the effects of confinement and a maximum compressive strain of 0.0038, exceeded the column moment corresponding to development of M_p in the beams. Column flexural strengths exceeded the flexural demands by 40 and 83 percent in Specimens J1 and J2, respectively. Column shear forces corresponding to the development of M_p in the beam were 235 and 244 kN (52.8 and 54.9 kips) for Specimens J1 and J2, respectively.

The calculated ratio of column flexural strength to beam flexural strength, based on measured material properties and dimensions and considering an equivalent rectangular stress block for the concrete as well as assuming that plane sections remain plane, was 1.53 and 2.08 for Specimens J1 and J2, respectively.

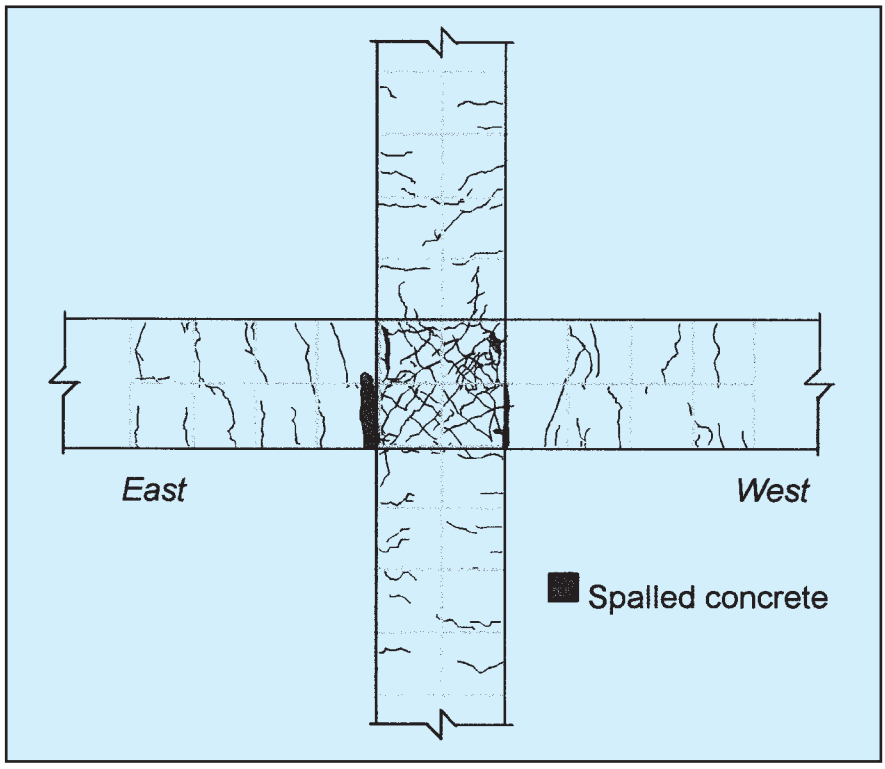

Fig. 6a. Crack pattern of Specimen J1 at design drift of 2 percent.

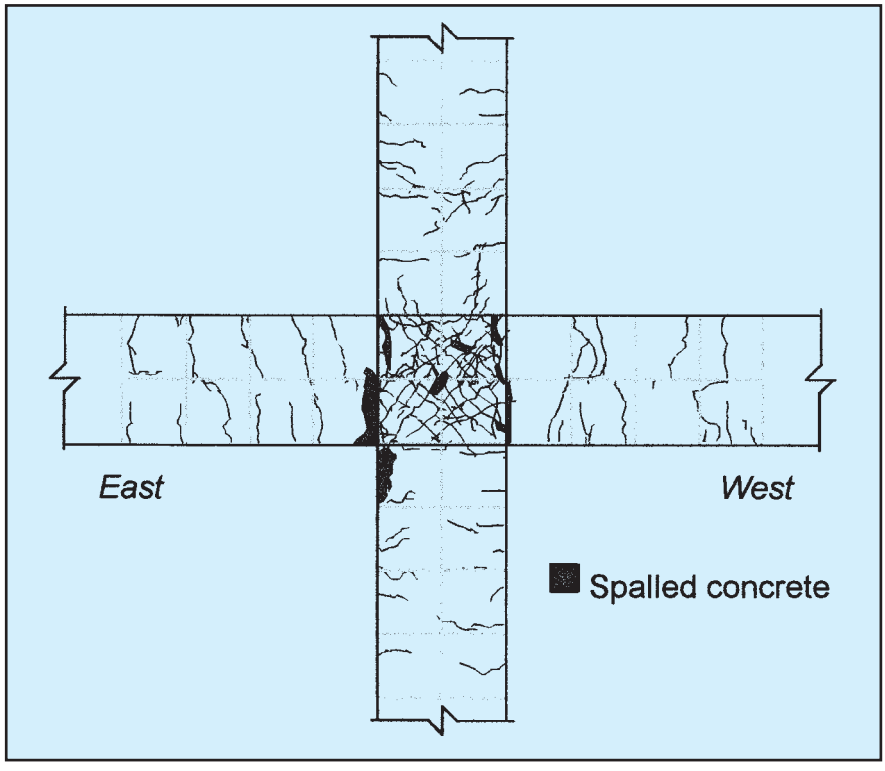

Fig. 6b. Crack pattern of Specimen J1 at maximum drift of 3.5 percent.

The joint shear forces and strengths are listed in Table 2. The horizontal shear forces were calculated assuming yielding of the beam top and bottom reinforcement and considering the column shear force. The joint shear stress was obtained by dividing the joint shear force by the column area. The shear stress at development of M_p in the beam hinges was 6.5 MPa (949

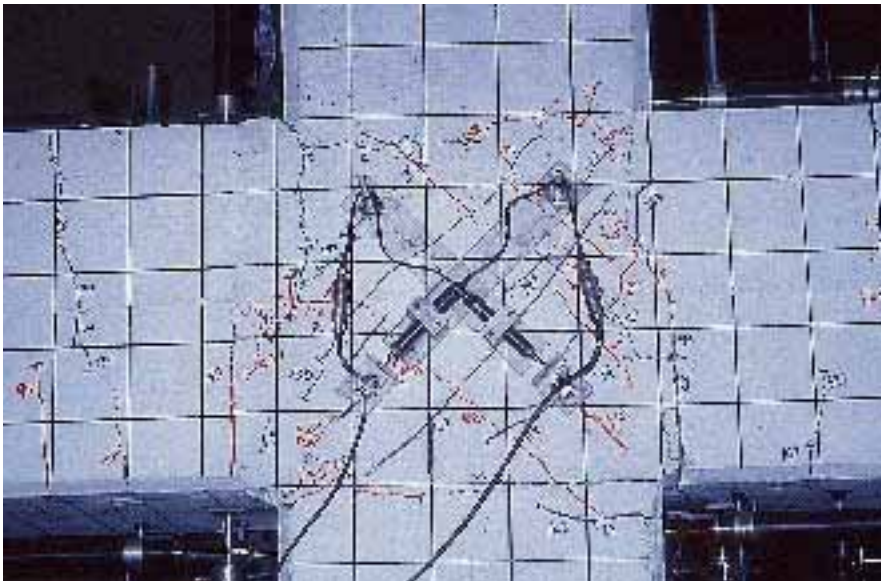

Fig. 7a. Joint damage of Specimen J1 at design drift of 2 percent.

psi), which corresponds to $0.99\sqrt{f_c'}$ MPa ($11.9\sqrt{f_c'}$ psi).

The joint shear strength was based on the shear strength recommended in ACI 352R,[22] which is the basis of the requirements in the MCBC. Since the joint was not effectively confined on all four vertical sides, a constant γ equal to 1 in MPa units (or 12 in psi units) was used to determine the stress at the shear strength, $\gamma\sqrt{f_c'}$.

Such recommendations are, in effect, applicable to monolithic construction, but were applied to these cases for comparison purposes. Therefore, it was expected that a diagonal strut would resist the entire horizontal joint shear introduced. Based on the experimental results, mechanisms involved in the joint shear transfer are discussed in more detail later in this paper.

Compliance with MCBC

Design and detailing complied with most requirements for precast construction and monolithic ductile frames in the MCBC.[6] The MCBC has design and detailing requirements for SMRFs that are similar to those of Chapter 21 of ACI 318-95[21] and of the Uniform Building Code.[7] Three design requirements prescribed in the MCBC were intentionally not fulfilled in the specimens.

1. Prestressing strands with a nominal yield stress greater than 414 MPa (60 ksi) provided continuity at the joint of Specimen J2.

2. Nominal joint shear strength capacities and joint shear demands were made approximately equal in both test units. As is preferred in earthquake-resistant design, specimens were designed and detailed to achieve ductile post-elastic deformations by flexural yielding in beam plastic hinges at the face of the column. However, high shear demands in the joint were purposely introduced in order to assess the beam-to-column joint shear capacity. Thus, while the longitudinal steel arrangement of columns was designed to reduce the likelihood of yielding, beam reinforcement and detailing were designed to ensure plastic hinging and to impose large shear force demands into the joint.

3. The 1.3 factor, specified by the MCBC to augment the moments and forces obtained from analyses (in addition to the usual load factors), was not included in the design of the test units. This was done because the specimens did not represent any prototype structure that would have been designed in accordance with the MCBC. In contrast, it was the one objective of the program to understand the joint load-carrying mechanisms and to assess the joint capacity. It should be emphasized that in all structures designed in Mexico City with the connections described herein, the 1.3 factor must be used.

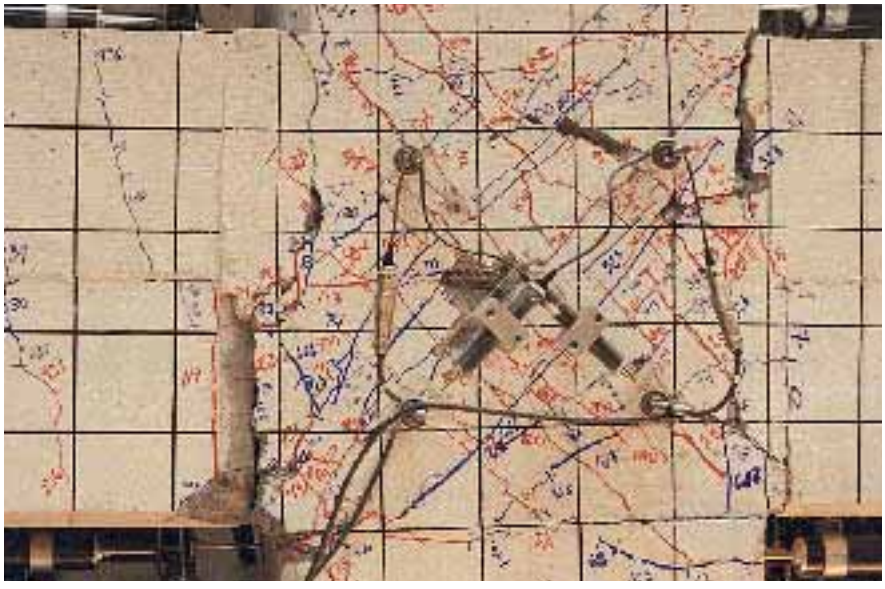

Fig. 7b. Joint damage of Specimen J1 at maximum drift of 3.5 percent.

TEST SETUP, LOADING PROGRAM, AND INSTRUMENTATION

The experimental setup for Specimens J1 and J2 is shown in Fig. 2. Column ends and beam ends were pinned. Horizontal displacements were applied at column midheight above the joint through a pin-ended double-acting actuator with the test unit rotating about a spherical bearing at the lower column midheight. The beams were connected at midspan positions to the reaction floor through pin-ended steel struts, allowing free

lateral translation of the beams but restraining vertical movement and ensuring a moment pattern in the specimen similar to that in a joint of a building frame under cyclic lateral loads. No axial load was applied to the columns since experimental evidence suggests that axial load has no effect on the joint shear strength.[23]

Specimens were tested under a displacement-controlled cyclic load history that was based on the interstory drift which represented a severe load condition for a beam-to-column joint (see Fig. 5). The test pattern is based on drift rather than ductility increments because ductility can be difficult to define for systems incorporating components other than conventionally reinforced concrete or mild reinforcing steel components.[14]

The loading sequence originated from recommendations made in a 1997 draft of the ITG document.[3] At each drift level, three cycles were applied. Bi-directional cycles up to 1.5, 2.5, and 3.5 percent drift were applied to Specimen J2, with the main loading direction being east-west (beam with square cross section). Specimens were subjected to much larger drifts than their design drift capacities of 2 percent.

Specimens were instrumented with displacement, strain, and load transducers.[19,20] Displacement transducers were attached to the beam and column surfaces at opposite faces to measure the axial deformations and calculate member rotations and curvatures. A set of transducers was placed in the joint region to obtain joint shear deformations. Resistive strain gauges were bonded to longitudinal and transverse reinforcing bars of columns and beams. A dense array of strain gauges was placed on the reinforcement of the joint details tested, as well as on the joint confining steel.

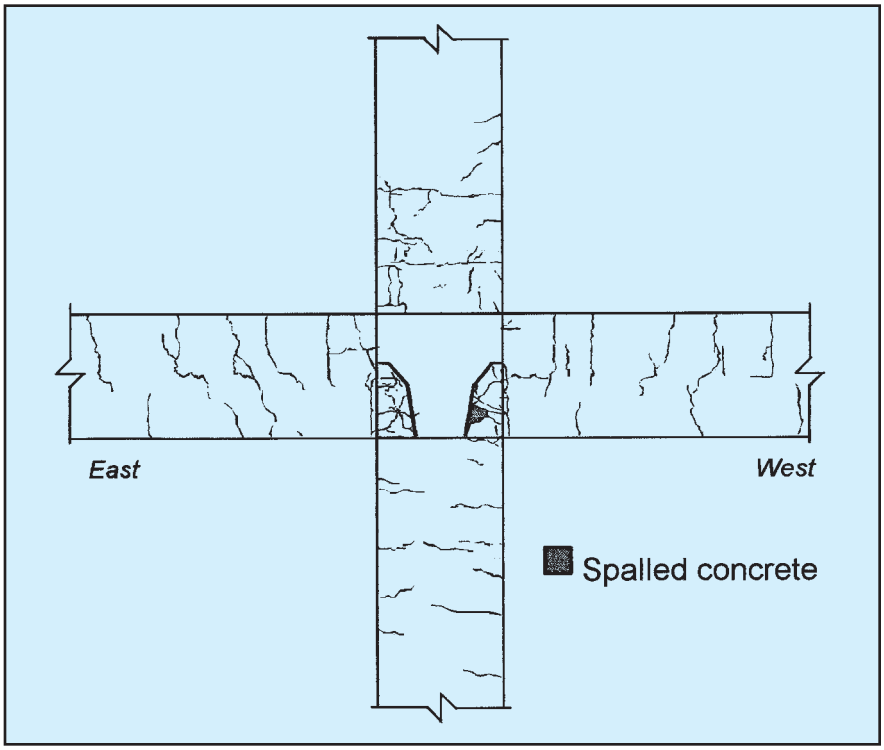

Fig. 8a. Crack pattern of Specimen J2 at design drift of 2 percent, east-west direction.

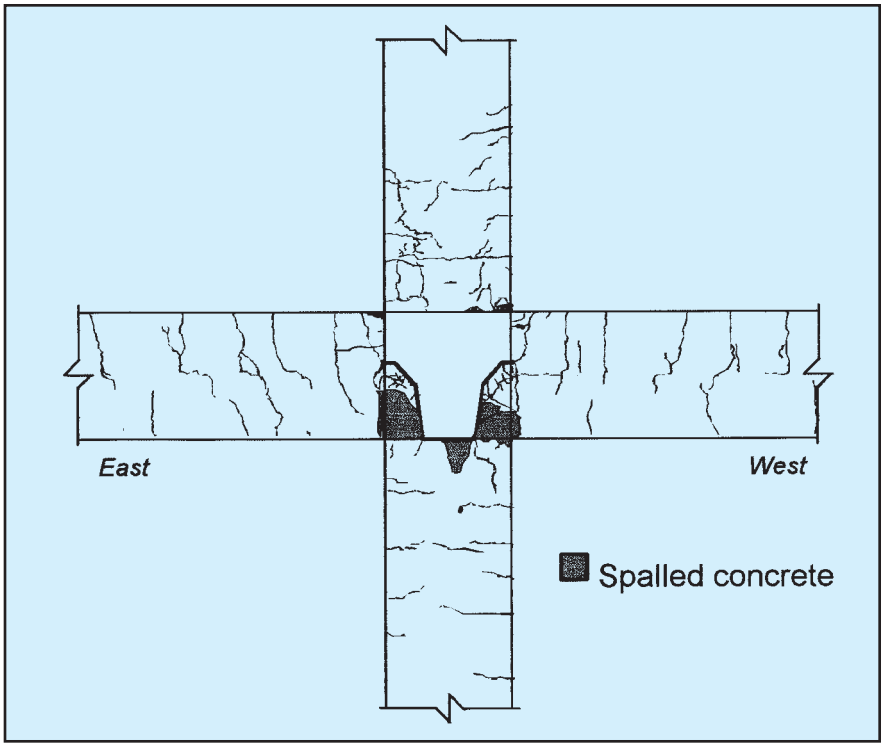

Fig. 8b. Crack pattern of Specimen J2 at maximum drift of 3.5 percent, east-west direction.

TEST RESULTS

The detailed test results, together with a discussion of the important points, are presented in this section.

Cracking Patterns

The crack patterns and photographs of joint damage at the design drift of 2.0 percent and at the end of the test are shown in Figs. 6 through 9 for Specimens J1 and J2. In both structures, most of the damage was concentrated in the joint and in the beams. Consistent with a strong-column–weak-beam system, the column damage was minor.

For Specimen J1 (see Figs. 6 and 7), the beams exhibited few flexural cracks near the column face. Spalling of cover concrete first developed at a

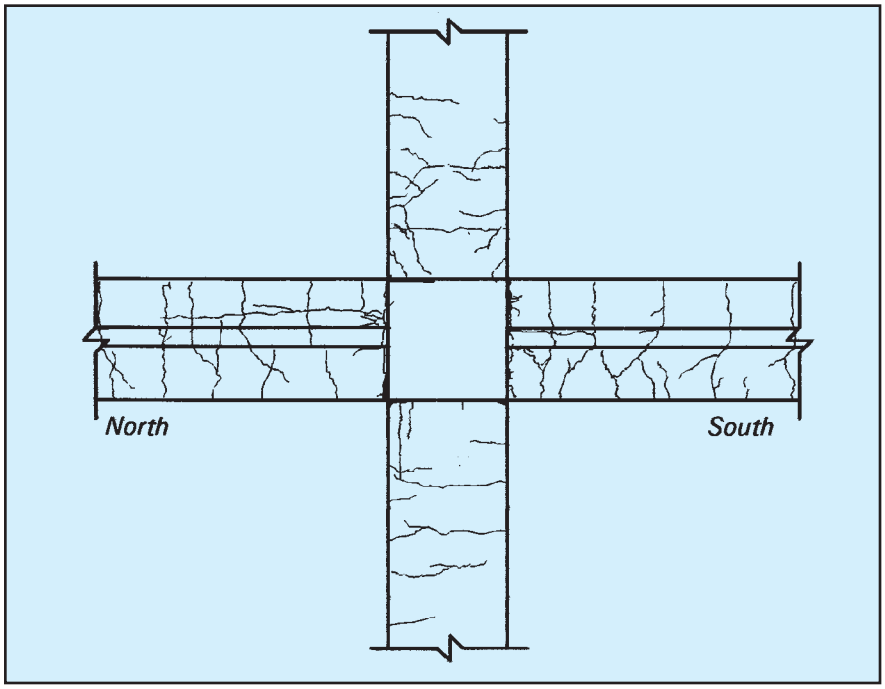

Fig. 8c. Crack pattern of Specimen J2 at maximum drift of 3.5 percent, north-south direction.

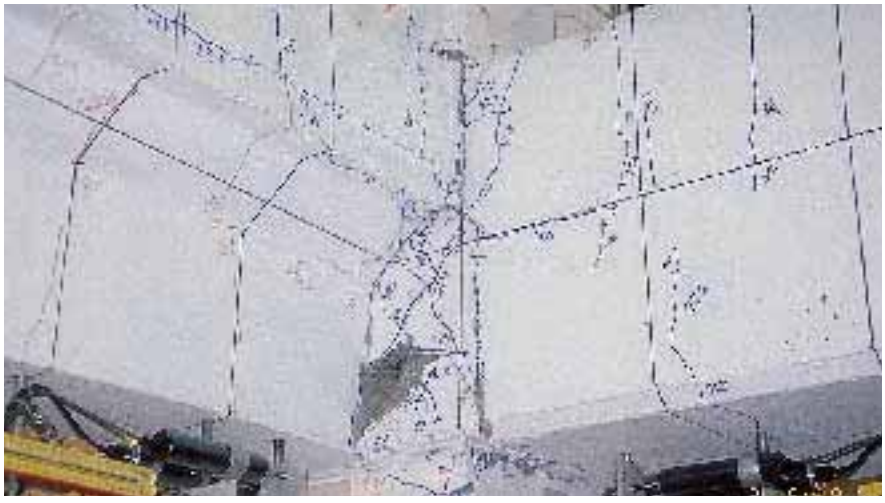
Fig. 9a. Joint damage of Specimen J2 at design drift of 2 percent, east-west direction.

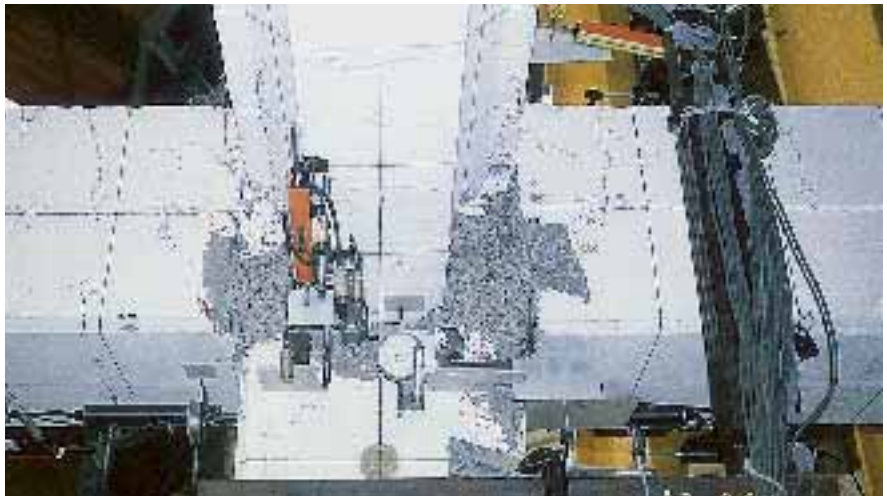
Fig. 9b. Joint damage of Specimen J2 at maximum drift of 3.5 percent, east-west direction.

drift of 3.0 percent; spalling progressed as drift increased. Under negative bending moment (top fibers in tension), a single vertical 10 mm (0.39 in.) wide crack at the column face occurred. Under positive bending moment, a 14 mm (0.55 in.) wide crack was observed at the column face following the contour of the precast concrete beam.

During specimen demolition, inclined cracking of the narrower portion of the beams inside the joint was observed. Such damage extended from the interior of the joint, at the lower side of the column gap, up and out to the beams. This damage is attributed to pullout of the beam bottom bars and beam rotation inside the joint that was not concentrated at the column face, as is commonly expected in monolithic construction. Also, the extent of beam damage at maximum drift (3.5 percent) was less than would be expected in monolithic reinforced concrete construction.

Column flexural cracking initiated at a drift of 0.5 percent and remained minor for the remainder of the testing. First joint inclined cracking developed at a drift of 0.25 percent. Considerable joint inclined cracking took place when cycling to drifts of 2.0 percent (see Figs. 6a and 7a). This extended up to a drift of 2.5 percent; the crack pattern stabilized and only a few cracks appeared at higher drifts. At maximum drifts, joint cracks were well distributed and oriented approximately parallel to the joint diagonal at a 45-degree angle (see Figs. 6b and 7b).

Specimen J2 showed cracking and damage patterns similar to Specimen J1 (see Figs. 8 and 9). Beams showed a more uniform distribution of cracking, especially under positive bending (top fibers in compression). The north-south beams exhibited cracking comparable to that observed in monolithic construction (see Fig. 8c). At similar drifts, beam crack widths in Specimen J2 were smaller than in Specimen J1.

At the design drift of 2.0 percent, no spalling was observed in the beams and only light spalling was observed in the joint region (see Figs. 8a and 9a). Joint inclined cracking first appeared at a drift of 0.25 percent. Cracking ex-

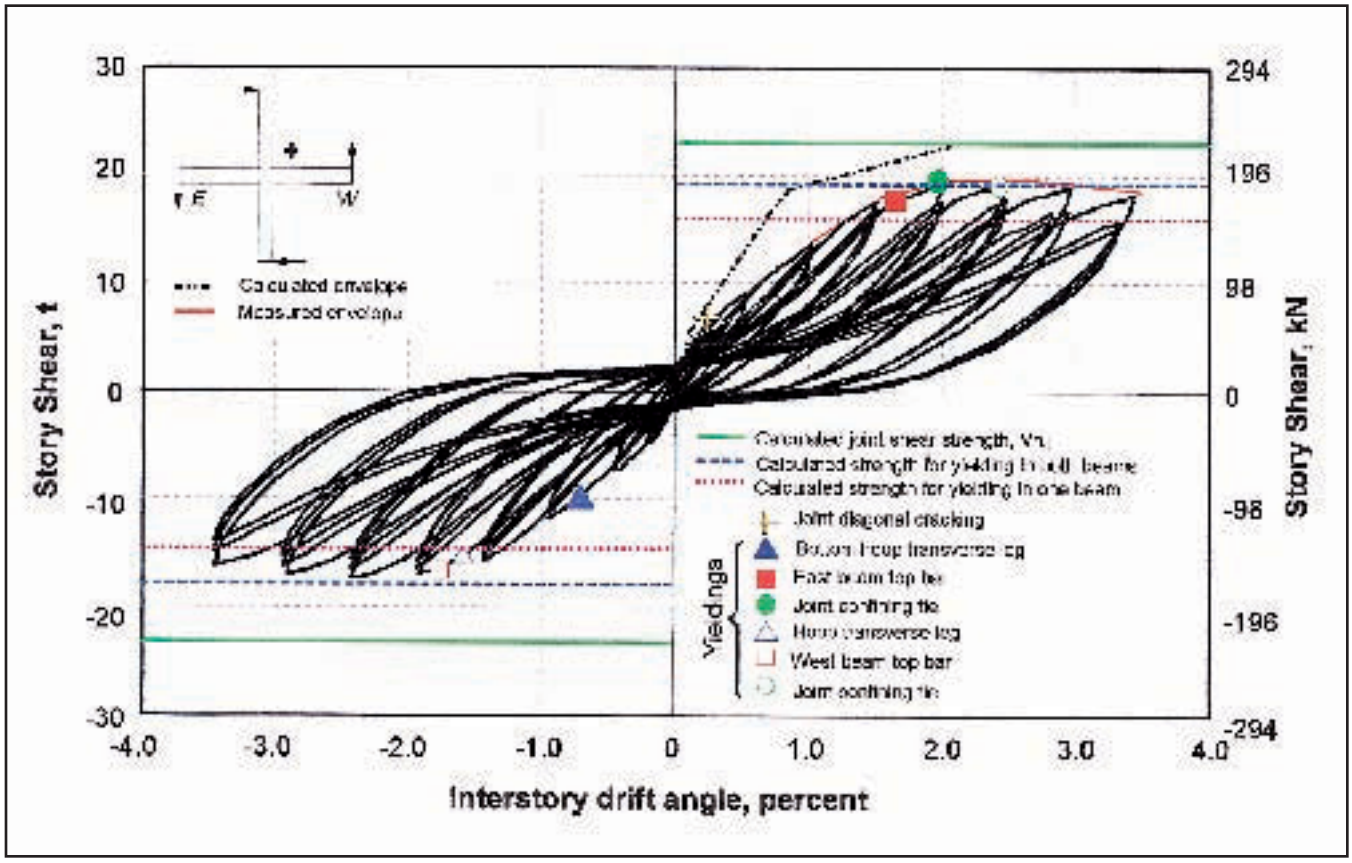

Fig. 10a. Story shear versus interstory drift for Specimen J1.

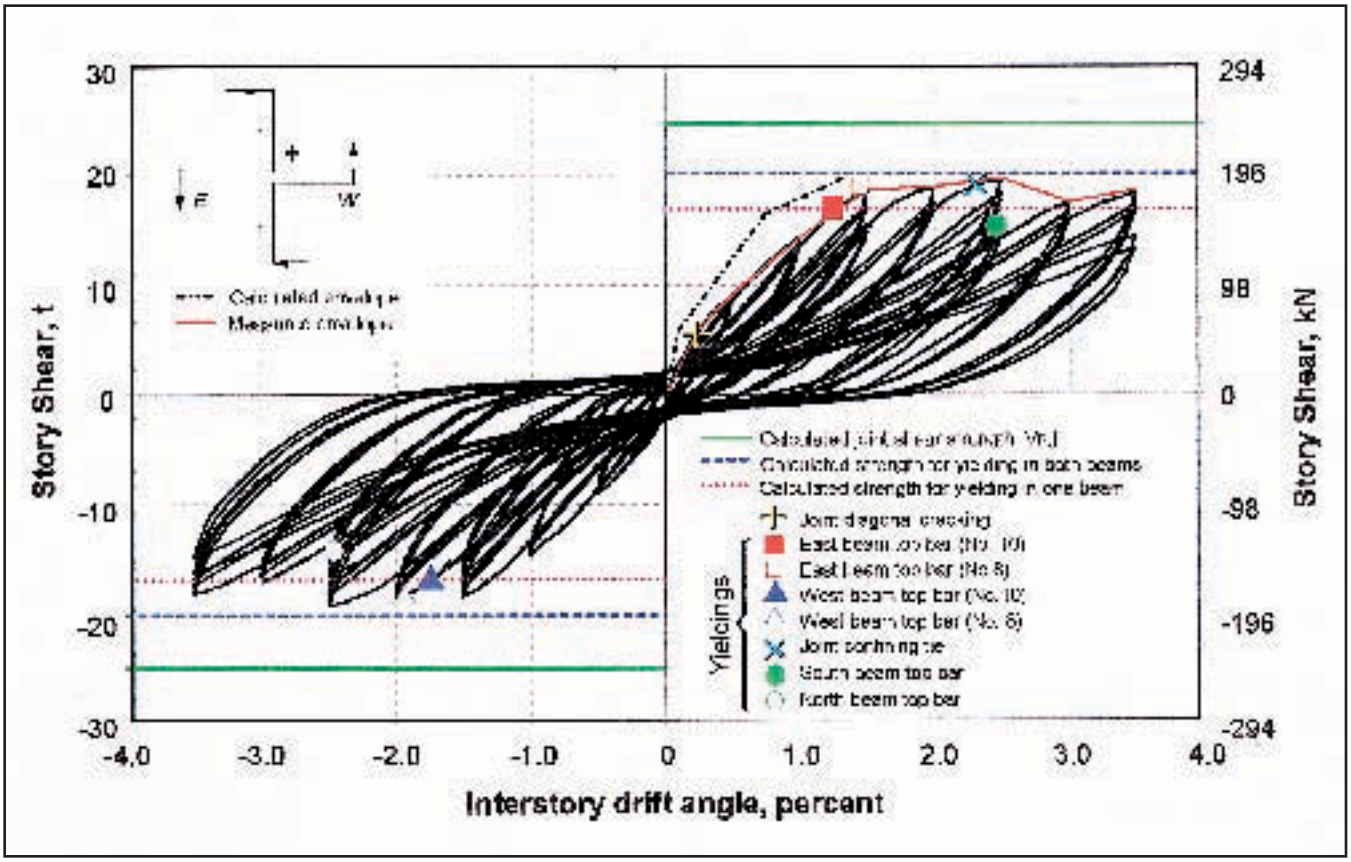

Fig. 10b. Story shear versus interstory drift for Specimen J2, east-west direction.

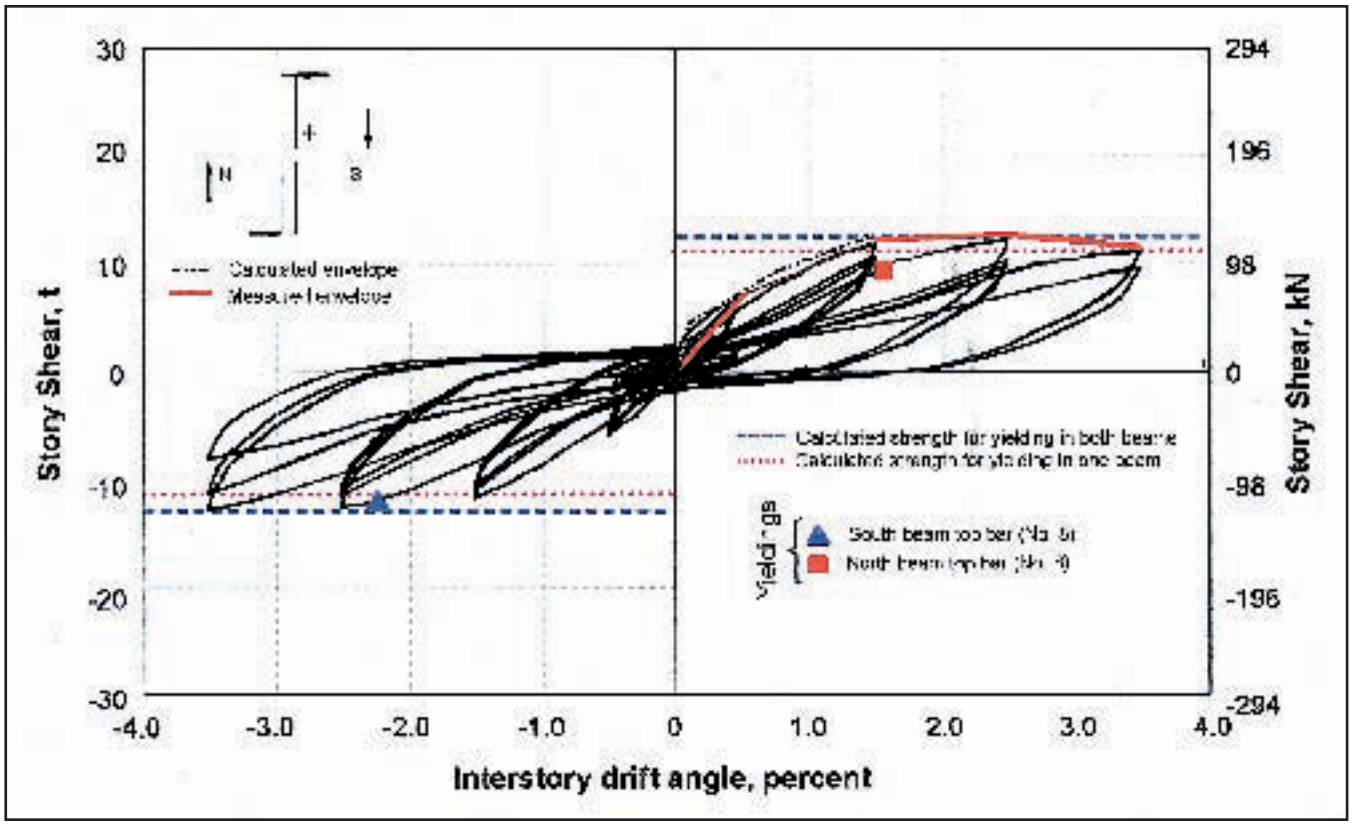

Fig. 10c. Story shear versus interstory drift for Specimen J2, north-south direction.

tended until a drift of 0.5 percent, after which it stabilized. At the same drifts, joint inclined cracks in Specimen J2 were finer than in Specimen J1. Spalling of the joint cover concrete occurred at 3.0 percent drift. Similarly to Specimen J1, under positive bending, the beam rotated inside the joint.

Story Shear Versus Interstory Drift

The hysteresis curves for story shear versus interstory drift for Specimens J1 and J2 are presented in Fig 10. The components of the bi-directional cycles of Specimen J2 in the east-west and north-south directions are presented in Figs. 10b and 10c. The story shears corresponding to joint failure, $V_{n,j}$, are also shown. The story shears corresponding to joint failure were based on the shear strength recommended by ACI 352R[22] (see Table 2).

The story shears associated with the formation of one or two plastic hinges in the beams are indicated as horizontal dashed lines. The occurrences of the first joint diagonal cracking and yielding recorded at several locations during the tests are also indicated in the figures. All of the recorded yielding took place at the face of the column.

The experimental response indicated a hysteretic behavior at drifts to 2.0 percent with comparatively low strength degradation among successive cycles at equivalent drift levels. The hysteresis loops are nearly symmetrical, even during bi-directional loading of Specimen J2. Considerable pinching and severe stiffness degradation is noticeable, especially at drifts of 3.5 percent. The hysteresis curves of Specimens J1 and J2 are dominated by the response of the most damaged elements, which were the joints and the beams.[19,20]

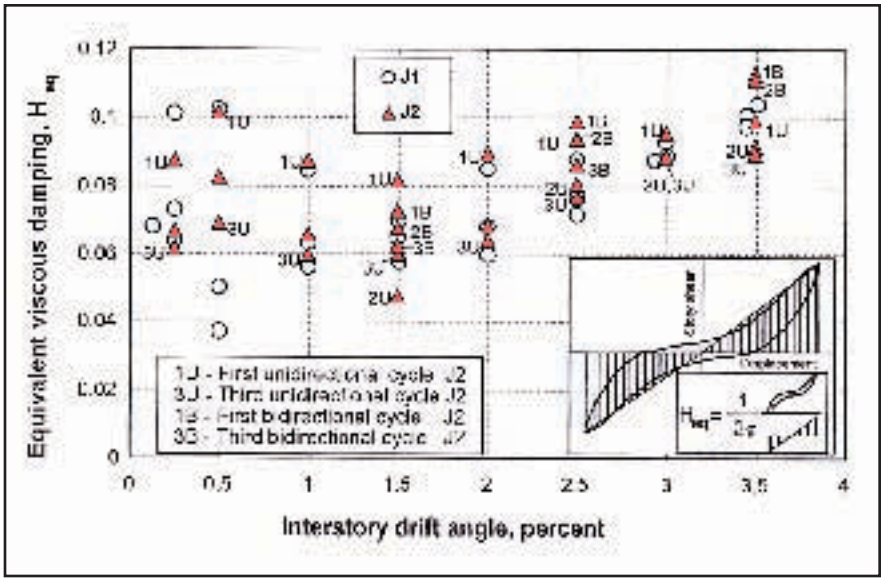

Fig. 11. Equivalent viscous damping versus interstory drift, east-west direction.

To assess the energy dissipation capacity and the stability of the hysteretic behavior, the equivalent viscous damping ratio, H_{eq}, was plotted against the interstory drift during east-west loading for both specimens (see Fig. 11). In the plot, H_{eq} was taken as the ratio of the dissipated energy within a cycle to 2π times the strain energy measured at peaks of an equivalent linearly elastic system.

In general, damping ratios increased with drift. At equivalent drifts, damping ratios decreased as much as 20 percent. This reduction is attributed to pinching in the curves; concrete damage and shear distress contributed to narrowing the hysteresis loops. Damping ratios for bi-directional cycles were higher.

Since the story shears were limited by the beam flexural strength and, more exactly, by pullout of the beam bottom bars, the calculated story shears corresponding to joint strength, $V_{n,j}$, in the east-west and north-south directions for Specimens J1 and J2 were never reached even at cycles to 3.5 percent drift. Measured strengths of Specimens J1 and J2 were about 80 percent of those expected in a monolithic beam-to-column connection designed according to ACI 352R[22] (see Fig. 10).

The calculated strength at first yielding in the specimens is related to yielding of the beam bottom longitudinal bars. In Specimen J1, the system reached the story shear associated with yielding not because the bottom bars had yielded, but because the connecting hoops had yielded. In Specimen J2, the bottom bars did not yield either, but because the top bar load path was much stiffer than the bottom one, the top bars reached strains within the strain-hardening zone.[19,20]

Analysis of the strain gauge data indicated that beam top steel bars yielded prior to achieving the specimen strength and before damage concentrated in the joint.[19,20] In Specimen J2, the maximum recorded steel strains were greater than 0.014. Bottom longitudinal steel bars of the beams remained elastic. Strains recorded on the joint continuity reinforcement are discussed later in the paper.

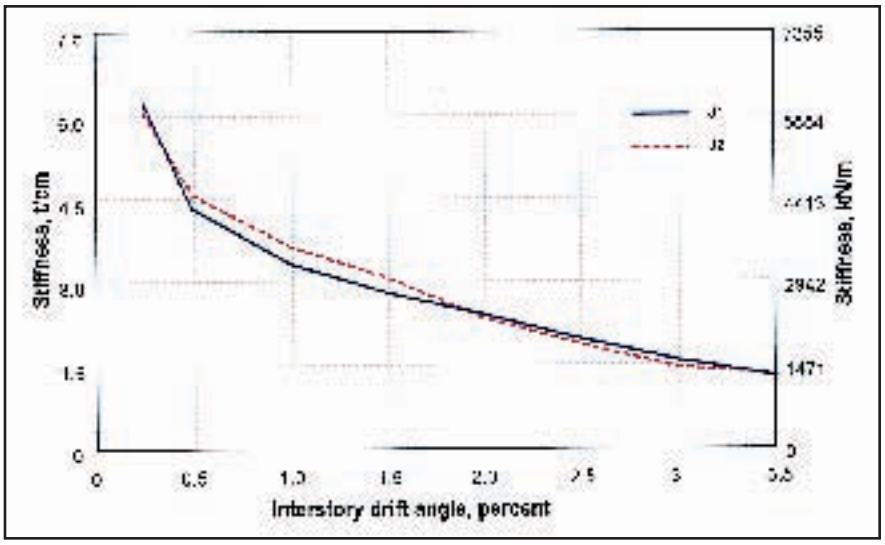

Fig. 12. Secant stiffness versus interstory drift angle.

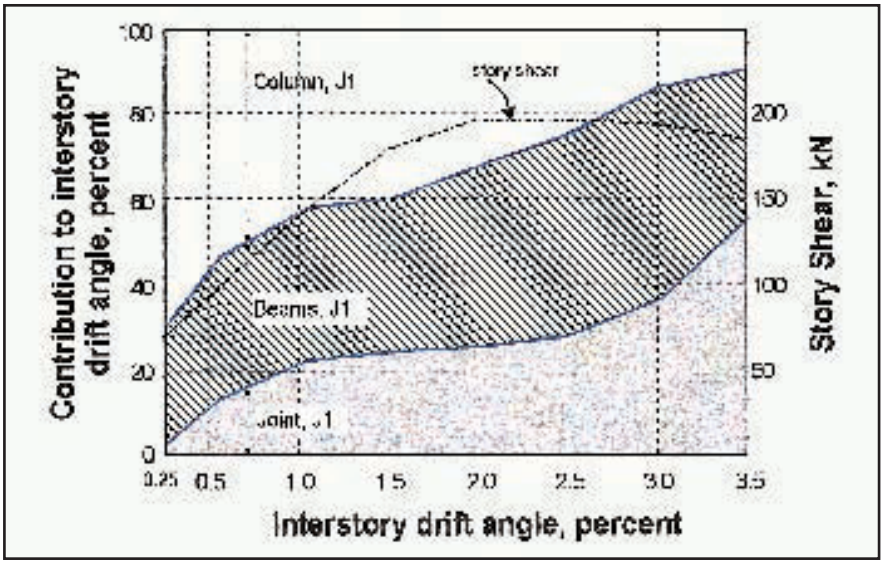

Fig. 13a. Member contribution to interstory drift for Specimen J1, east-west direction.

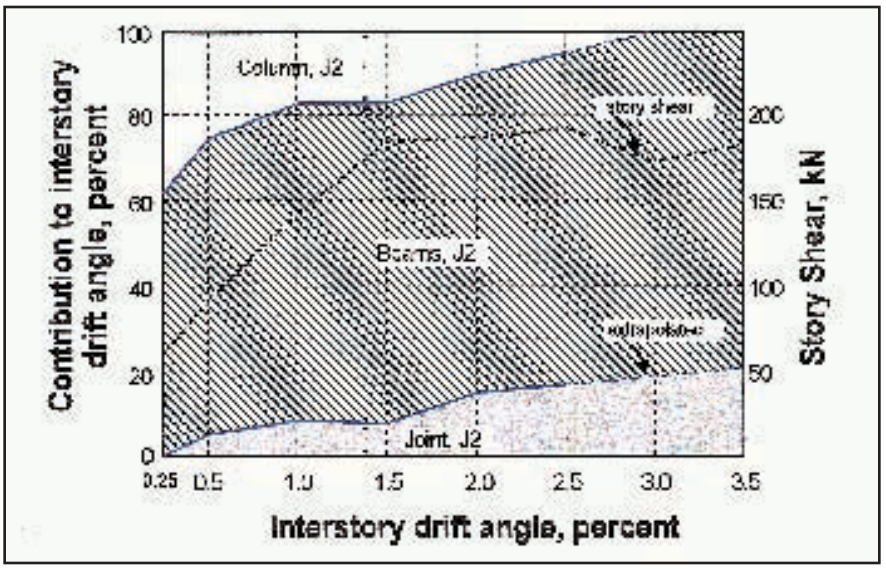

Fig. 13b. Member contribution to interstory drift for Specimen J2, east-west direction.

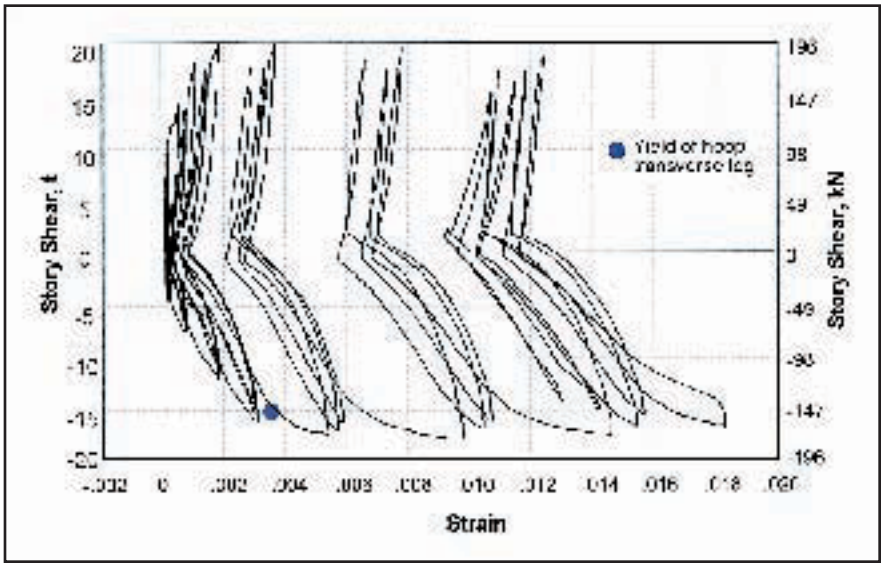

Fig. 14. Strain on transverse leg of a continuity hoop of Specimen J1.

Response Envelopes

Calculated story shear–drift response envelopes of Specimens J1 and J2 are also shown in Fig. 10. Beam flexural behavior was assumed to control the specimen response when the envelopes were calculated. The effect of strain hardening of the beam longitudinal reinforcement on specimen strength, stiffness, and inelastic deformability were taken into account in Specimen J1.

For Specimen J2, the calculation only considered the contribution to flexural strength of strand yielding, whereas in the beam top reinforcement, the effect of strain hardening at the column face was considered.

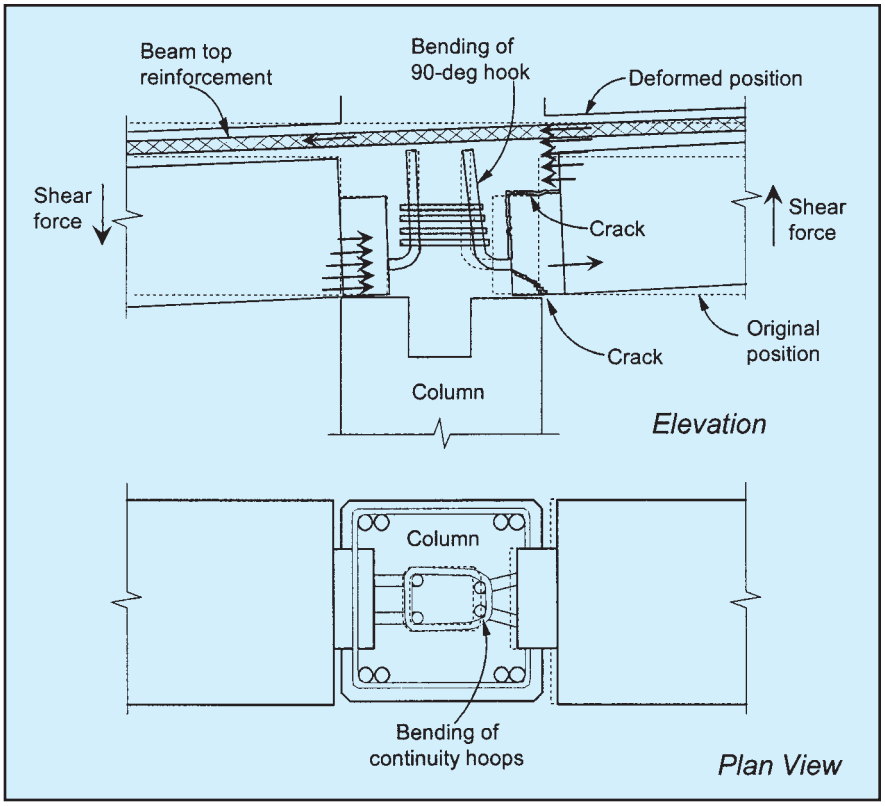

Fig. 15. Proposed plastic mechanism at failure of Specimen J1.

The measured initial lateral stiffnesses of the specimens were one-half of the calculated values. Calculated stiffnesses were based on elastic and monolithic behavior, as well as on uncracked sections. For Specimen J1, the calculated response showed higher strength and stiffness; this is also noticeable at large drift levels since strain hardening and concrete confinement were considered in the prediction. Analysis of the strain gauge data did not reveal any evidence of strain hardening of the beam longitudinal reinforcement, nor any significant improvement of concrete characteristics in the beams next to the column due to confinement.[19]

For Specimen J2, the measured envelope in the east-west direction indicated less stiffness and strength than the calculated curve. However, the difference between the actual and calculated responses was less pronounced than those of Specimen J1. This was believed to indicate that conventional mild steel beam bottom reinforcement (Grade 60) was mobilized. Indeed, strain gauge analysis further confirmed this reasoning.[20] In the north-south direction of Specimen J2, agreement between measured and calculated envelopes was acceptable.

Stiffness Deterioration

In order to assess stiffness deterioration, the secant stiffness was computed for each loading cycle. The secant stiffness was calculated using a straight line drawn between the maximum load and corresponding drift points for the positive and negative directions in a loading cycle (peak-to-peak stiffness).

Both specimens exhibited a similar initial lateral peak-to-peak stiffness and a comparable rate of stiffness deterioration (see Fig. 12). At a drift of 2.0 percent, Specimens J1 and J2 had retained 40 percent of their initial peak-to-peak stiffness. This value compares favorably with ungrouted post-tensioned beam-to-column joints[14] and with monolithic connections.[23] The different joint detailing used to achieve continuity of beam reinforcement in Specimens J1 and J2 did not affect the trend observed.

Member Contribution to Interstory Drift

The relative components of interstory drift (beam and column flexural and shear deformations, and joint distortion) were calculated.[19,20] Member contributions to drift during east-west positive cycles are shown in Fig. 13. Note that the variation of measured story shear is also shown. The story shear indicates the effect of the changes in a given portion of the structure on the strength of the specimen, and is particularly important in understanding the mode of failure.

For both specimens, the columns contributed least to total deformation. For Specimen J1, after cycles to 2.5 percent, joint deformations contributed more to the total drift. This is consistent with the damage observed in the joint. For Specimen J2, beams contributed the most to total deformation. Although the joint contribution was smaller than in Specimen J1, its contribution increased steadily in cycles between 1.5 and 2.5 percent.

Since the data became unreliable after 2.5 percent due to spalling of the joint concrete, it is not possible to determine the final member contributions to total drift in Specimen J2. From the figures, it is clear that the story shears remained nearly constant to very large drifts, despite the fact that the joint contributed significantly to total drift. The ductile failure observed is explained by yielding of the continuity hoops (in Specimen J1) and bar pullout (in Specimens J1 and J2) inside the joint. Such mechanisms caused the joint softening.

Strains in the Continuity Reinforcement Within the Joint

As previously mentioned, the beam bottom reinforcement in Specimen J1 was made continuous through the joint by a set of four No. 5 hoops placed around the extensions of the 90-degree hooks that protruded from the beam ends. The hoops were designed to remain elastic when the maximum tensile force in the bottom reinforcement corresponding to the beam flexural strength was developed. Strain gauges were bonded on hoop legs in directions parallel and orthogonal to the loading direction (east-west direction).[19]

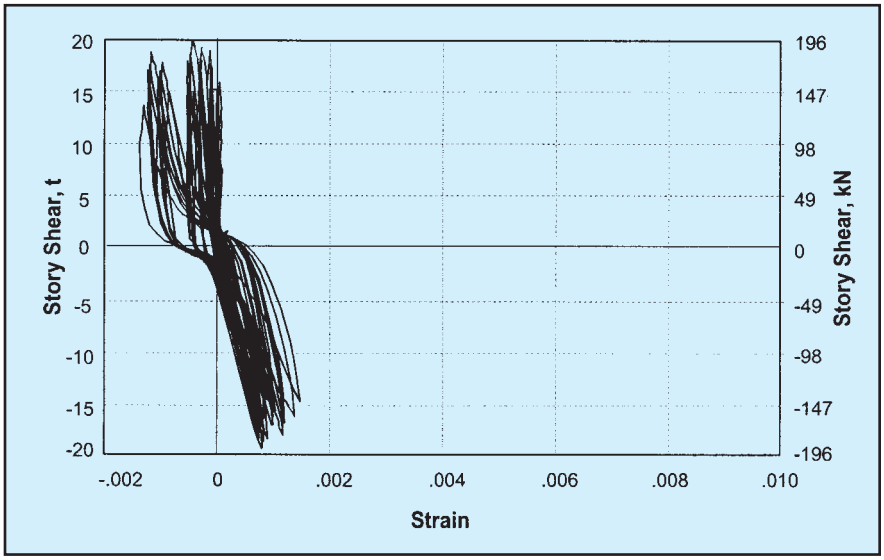

Fig. 16. Strain on No. 12 vertical bar at beam soffit section of Specimen J2.

Strains recorded in the continuity reinforcement demonstrated the bending flexibility of the transverse legs (parallel to the north-south direction) of hoops when the 90-degree hook extensions tried to pull away from the joint. From the early stages of the test (see Fig. 14), the high bending flexibility of the transverse legs increased the beam rotation, concentrating it inside the joint.

Subsequent plastification under bending further contributed to centering the rotation inside the joint and softening the joint core. The pullout failure mechanism of the beam hooked bar in the joint caused the inclined cracking observed in the narrow portion of the beam inside the joint which was mentioned earlier. The proposed plastic mechanism at failure of Specimen J1 is depicted in Fig. 15.

The precast beam bottom reinforcement of Specimen J2 was made continuous through the joint by means of a No. 12 Grade 60 bar placed vertically in the intersection of the four looped 12.7 mm (0.5 in.) diameter, Grade 270 prestressing strands that protruded from the beam ends.

Strains recorded in the vertical No. 12 bar at the beam soffit section and in the east looped strand at the beam end section (inside the joint) are shown in

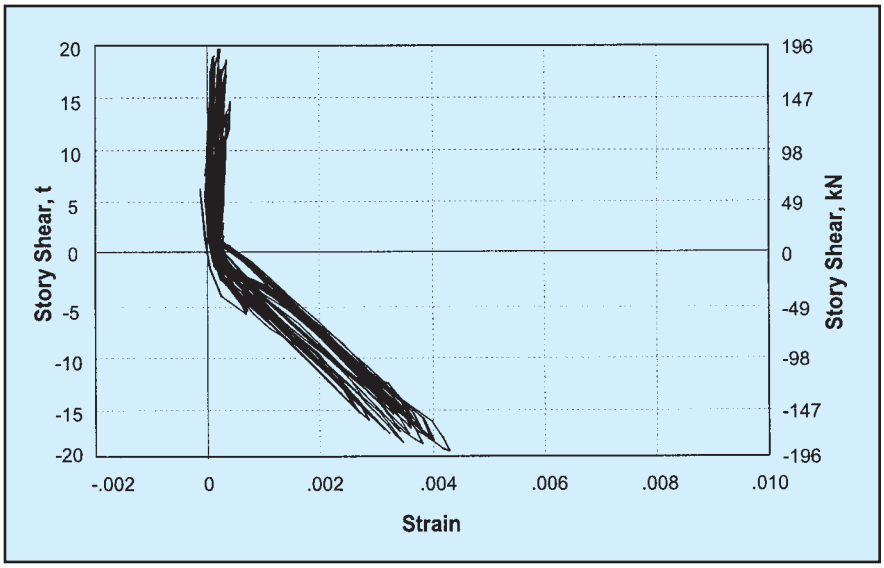

Fig. 17. Strains on east looped strand at beam end section of Specimen J2.

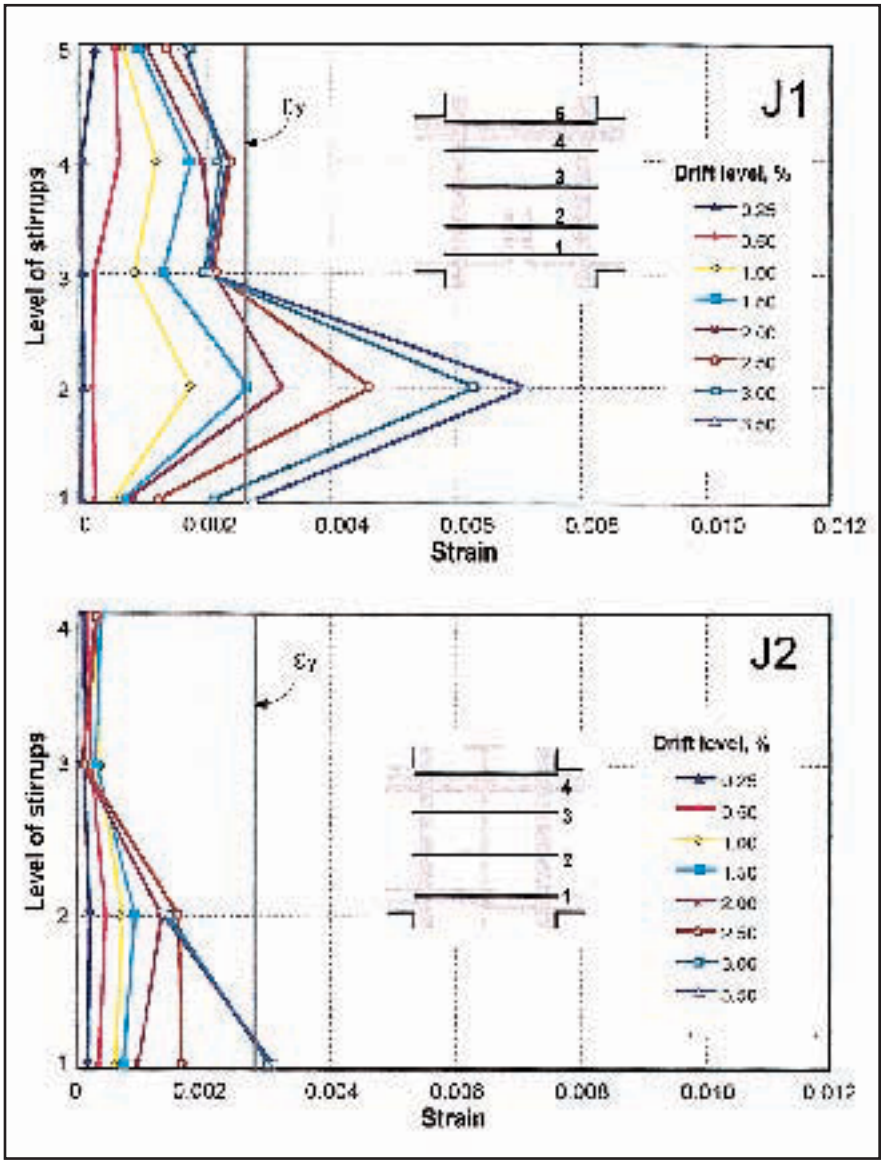

Fig. 18. Joint hoop strains for Specimens J1 and J2.

Figs. 16 and 17, respectively. Although the No. 12 bar, looped strands, and bottom beam bars remained elastic, damage patterns and hysteretic behavior comparable to those of Specimen J1 were observed. It is believed that the continuity joint reinforcement of Specimen J2 was not stiff enough to preclude the beam from rotating inside the joint under positive bending, as was observed during the test of Specimen J2.

Clearly, the joint behavior of Specimens J1 and J2 was negatively affected by the beam rotation inside the joint. The internal mechanisms of resistance (the main diagonal concrete strut and truss actions), joint stiffness and toughness were harmed by the development of a tensile strain field that cracked the joint concrete early in the test.

Joint Hoop Strains

Strains developed in the confining steel bars parallel to the loading direction within the joint height are shown in Fig. 18. Results for Specimen J1 indicate that Positions 1 and 2 sustained strains exceeding yield at drifts larger than 2.0 percent, with first yield being recorded at 2.0 percent drift. Strains close to $3e_y$ were recorded at maximum drift. The largest strains measured within the lower half of the joint are consistent with strains developed due to the pullout of beam bottom bars.

In contrast, strains recorded in Specimen J2 were much lower than for Specimen J1, with maximum values of about $1.5e_y$. Except for the bar in Position 1, all confining bars remained elastic.

Joint Force Transfer Mechanism

In order to understand the mechanism involved in joint shear transfer, strain gauge data for Specimens J1 and J2 were investigated in more detail. From "measured" forces in bars (calculated from strains and a cyclic stress-strain model curve), several strut-and-tie models were analyzed. Possible strut-and-tie models for the two specimens are shown in Figs. 19a and 19b. Column forces at each bundle of reinforcing bars were calculated from moment-curvature analyses using the column flexural moments corresponding to the applied lateral shear force. From Figs. 19a and 19b, column and beam flexural compression resultants combine to form a diagonal strut. Hoop tensile forces, considered to be lumped at joint midheight, are equilibrated at the core boundary by two inclined struts angling towards the centroid of the beam and column compression resultants and by changes in the column reinforcing bar forces.

The inclined struts in the lower half of the joint are of particular interest. In Specimen J1, the strut (with 235 kN) is balanced horizontally by tensile forces in the continuity hoops and bond along the horizontal short segment of the bar protruding from the beam end, and vertically through bond along the hook extension of beam reinforcement. This mechanism is similar to that observed in pullout failures of bars. In Specimen J2, the horizontal reaction of the inclined strut is given by dowel action of the No. 12 bar placed to give continuity to the beam bottom reinforcement.

For the struts within the lower half of the specimen, premature cracking due to bar pullout softens the joint region, thus reducing its stiffness and resistance to shear forces. Such inclined cracks at the lower half are supported by the observed crack patterns of Figs. 6 and 8.

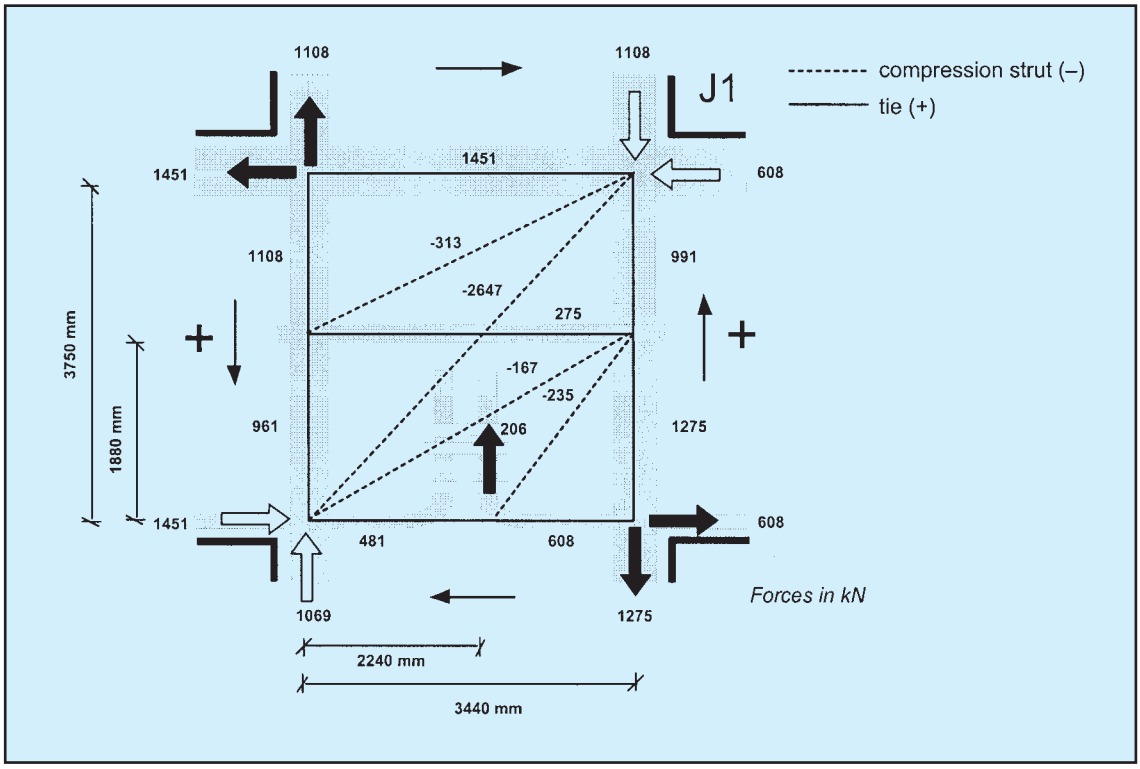

Fig 19a. Possible strut-and-tie model of joint region of Specimen J1 at strength.

It is possible, based on strut-and-tie models, to determine how much of the net force differential in the column bundled bars was transferred by strut-and-tie action involving the hoop sets and how much was transferred by shear-compression within the major diagonal strut. From Fig. 19a, for example, the force differential in the column bundled bars is 1108 + 1275 = 2383 kN (536 kips). As shown, hoop forces assist in transferring only 991 + 1275 = 2266 kN (509 kips), or 95 percent of the total. It can be inferred that the remainder, 2383 – 2266 = 117 kN (26 kips), was transferred by shear-compression within the width of the diagonal strut.

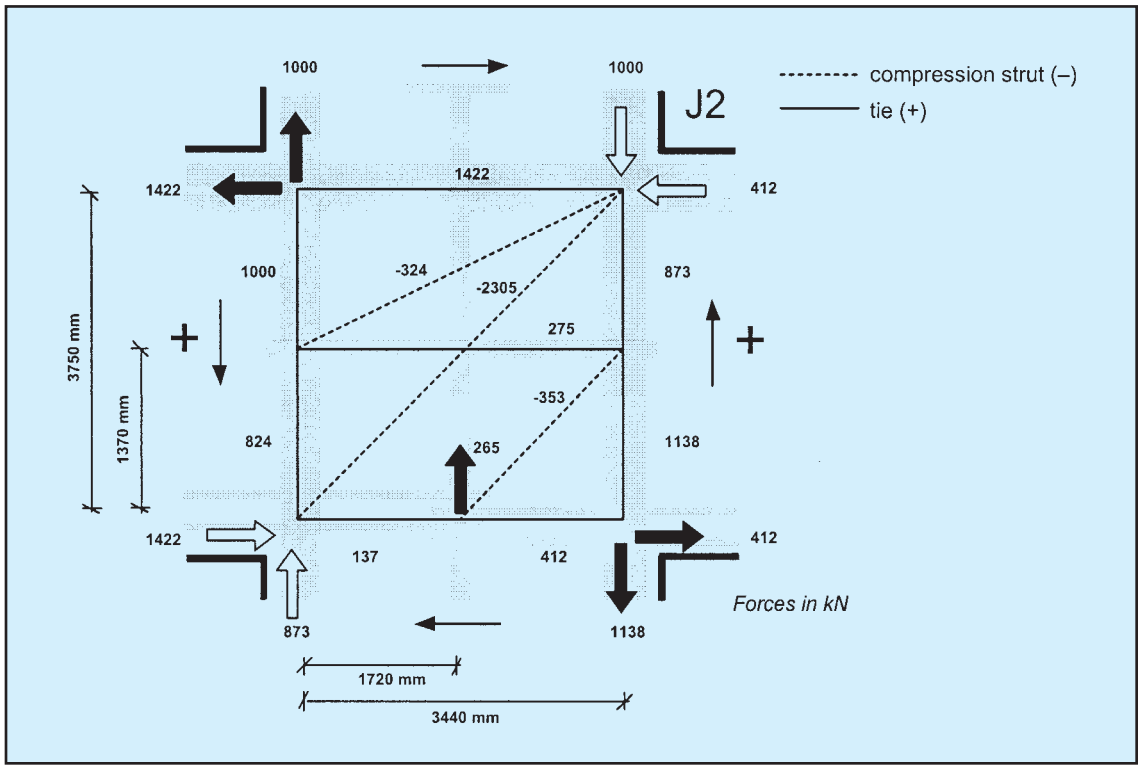

Fig 19b. Possible strut-and-tie model of joint region of Specimen J2 at strength.

CONCLUSIONS

Based on the observations and results during fabrication, testing, and data analysis of the two large-scale precast concrete beam-to-column connections, the following conclusions can be made:

1. Precast concrete frames using the two tested beam-to-column connections can be built easily and quickly.

2. The specimens exhibited ductile behavior. The lateral load carrying capacity was maintained nearly constant up to drifts of 3.5 percent, which are larger than the maximum drift values allowed in most design codes around the world.

3. The specimens were designed to develop plastic hinges in the beams next to the columns and to impose joint shear demands close to the nominal joint shear strength for monolithic construction. As expected, the behavior was controlled by the joint at large drifts. Joint degradation and stiffness decay were recorded after the beam top steel reinforcement of the beam had yielded in tension.

4. In both structures, beam rotation took place inside and outside the joint. Joint mechanisms of resistance were impaired by the development of tensile strains due to beam rotation inside the joint. Beam rotation inside the joint does not usually occur in monolithic construction.

5. In Specimen J1, where hoops were used to achieve continuity, premature bending flexibility of hoop legs transverse to the loading direction, as well as pullout of beam bottom bars, contributed to initial joint damage.

6. Specimen J2 (in which continuity of bottom longitudinal reinforcement of the beams is provided by a steel bar inserted through overlapping U-shaped prestressing strands) performed better than Specimen J1. Specimen J2 exhibited a more uniform distribution of beam cracking and yielding under negative bending.

7. Continuity reinforcement in the form of hoops or U-shaped strands should be sufficiently strong and stiff to avoid plastic behavior under maximum demands calculated from a capacity design approach.

8. Joint shear strengths of Specimens J1 and J2 were 80 and 90 percent, respectively, of those expected for monolithic construction. Moreover, the initial shear cracking occurred at lower levels of nominal shear stress than in monolithic construction. This phenomenon was attributed to premature beam rotation inside the joint.

9. The test results showed that the structural response of the precast frame was satisfactory. Although the connections tested did not fully emulate monolithic construction, they can be used in precast concrete frame systems or in hybrid systems, provided that their strength and stiffness are taken into account.

10. To improve the cyclic behavior of the connections, beam rotations inside the joint should be minimized. One approach to accomplishing this objective is to force the concentration of beam flexural rotations away from the column faces, i.e., relocate the beam plastic hinges. An alternative to reducing beam rotations inside the joint is to place unbonded post-tensioning tendons through the joint.

ACKNOWLEDGMENT

The support of the staff of the Large-Scale Structures Testing Laboratory of the National Center for Disaster Prevention (CENAPRED) and of Servicios y Elementos Presforzados, S.A. de C.V. (SEPSA) is gratefully acknowledged. This investigation is part of a research program sponsored by CENAPRED and SEPSA. The connection system is protected under U.S. Patent No. 5 682 717 and Mexican Patent No. 94/09263.

The authors wish to express their appreciation to the PCI JOURNAL reviewers for their constructive comments.

REFERENCES

1. Vasconez, R. M., Naaman, A. E., and Wight, J. K., "Review of Research on the Design of Ductile Beam-to-Column Connections for Precast Concrete Frames," Report No. UMCEE 94-33, Department of Civil and Environmental Engineering, University of Michigan, Ann Arbor, MI, October 1994, 173 pp.
2. Englekirk, R. E., "Seismic Design Considerations for Precast Concrete Multistory Buildings," PCI JOURNAL, V. 35, No. 3, May-June 1990, pp. 40-51.
3. ACI Innovation Task Group 1, "Acceptance Criteria for Moment Frames Based on Structural Testing," Provisional Standard, American Concrete Institute, Farmington Hills, MI, 1999.
4. Ghosh, S. K., Nakaki, S. D., and Krishnan, K., "Precast Structures in Regions of High Seismicity: 1997 UBC Design Provisions," PCI JOURNAL, V. 42, No. 6, November-December 1997, pp. 76-93.
5. Park, R., "A Perspective on the Seismic Design of Precast Concrete Structures in New Zealand," PCI JOURNAL, V. 40, No. 3, May-June 1995, pp. 40-60.
6. *Reglamento de Construcciones Para el Distrito Federal* (in Spanish), Departamento del Distrito Federal, Gaceta Oficial del Distrito Federal, México, D.F., 1997.
7. UBC, *Uniform Building Code,* International Conference of Building Officials, Whittier, CA, 1997.
8. Sucuoglu, H., "Effect of Connection Rigidity on Seismic Response of Precast Concrete Frames," PCI JOURNAL, V. 40, No. 1, January-February 1995, pp. 94-103.
9. Cheok, G. S., and Lew, H. S., "Performance of Precast Concrete Beam-to-Column Connections Subjected to Cyclic Loading," PCI JOURNAL, V. 36, No. 3, May-June 1991, pp. 56-67.
10. Cheok, G. S., and Lew, H. S., "Model Precast Concrete Beam-to-Column Connections Subjected to Cyclic Loading," PCI JOURNAL, V. 38, No. 4, July-August 1993, pp. 80-92.
11. Englekirk, R., "Development and Testing of a Ductile Connector for Assembling Precast Concrete Beams and Columns," PCI JOURNAL, V. 40, No. 2, March-April 1995, pp. 36-51.
12. Nakaki, S. D., Stanton, J. F., and Sritharan, S., "An Overview of the PRESSS Five-Story Precast Test Building," PCI JOURNAL, V. 44, No. 2, March-April 1999, pp. 26-39.
13. Palmieri, L., Saqan, E., French, C. W., and Kreger, M.E., "Ductile Connections for Precast Concrete Frame Systems," Paper No. SP162-13, Mete A. Sozen Symposium, ACI SP 162, American Concrete Institute, Farmington Hills, MI, 1996, pp. 313-355.
14. Priestley, M. J. N., and MacRae, G. A., "Seismic Tests of Precast Beam-to-Column Joint Subassemblages with Unbonded Tendons," PCI JOURNAL, V. 41, No. 1, January-February 1996, pp. 64-81.
15. Priestley, M. J. N., "The PRESSS Program – Current Status and Proposed Plans for Phase III," PCI JOURNAL, V. 41, No. 2, March-April 1996, pp. 22-41.
16. Restrepo, J. I., Park, R., and Buchanan, A. H., "Tests on Connections of Earthquake Resisting Precast Reinforced Concrete Perimeter Frames of Buildings," PCI JOURNAL, V. 40, No. 4, July-August 1995, pp. 44-61.
17. Restrepo, J. I., Park, R., and Buchanan, A. H., "Design of Connections of Earthquake Resisting Precast Reinforced Concrete Perimeter Frames," PCI JOURNAL, V. 40, No. 5, September-October 1995, pp. 68-80.
18. Kanoh, Y., "Review of Japanese Precast Concrete Frame Systems Used as Building Structures," Proceedings of a Seminar on Precast Concrete Construction in Seismic Zones, Japan Society for the Promotion of Science and National Science Foundation, Tokyo, Japan, V. 2, October 1986, pp. 35-54.
19. Alcocer, S. M., Perez-Navarrete, D., and Gomez, A., "Estudio del Comportamiento de Una Conexión Viga–Columna de Elementos Prefabricados - Modelo J-E-" (in Spanish), Report IEG/01/00, Centro Nacional de Prevención de Desastres (CENAPRED), Mexico, D.F., April 2000, 54 pp.
20. Alcocer, S. M., and Perez-Navarrete, D., "Estudio del Comportamiento de Una Conexión Viga–Columna de Elementos Prefabricados - Modelo J-T-" (in Spanish), Report IEG/02/00, Centro Nacional de Prevención de Desastres (CENAPRED), Mexico, D.F., July 2000, 73 pp.
21. ACI Committee 318, "Building Code Requirements for Structural Concrete (ACI 318-95)," American Concrete Institute, Farmington Hills, MI, 1995, 369 pp.
22. ACI-ASCE Committee 352, "Recommendations for Design of Beam-to-Column Joints in Monolithic Reinforced Concrete Structures (ACI 352R-91)," American Concrete Institute, Farmington Hills, MI, 1991, 18 pp.
23. Kurose, Y., Guimaraes, G. N., Zuhua, L., Kreger, M. E., and Jirsa, J. O., "Study of Reinforced Concrete Beam-to-Column Joints Under Uniaxial and Biaxial Loading," PMFSEL Report No. 88-2, Phil M. Ferguson Structural Engineering Laboratory, University of Texas at Austin, Austin, TX, December 1988, 146 pp.